Soft Computing (2020) 24:6809–6833
https://doi.org/10.1007/s00500-019-04316-5

METHODOLOGIES AND APPLICATION

Optimum design of shallow foundation using evolutionary algorithms

Ali R. Kashani[1] · Mostafa Gandomi[2] · Charles V. Camp[1] · Amir H. Gandomi[3]

Published online: 25 September 2019

Abstract
In the current study, the performance of three evolutionary algorithms, differential algorithm (DE), evolution strategy (ES), and biogeography-based optimization algorithm (BBO), is examined for foundation design optimization. Moreover, four recent variations of evolutionary-based algorithms [i.e., improved differential evolution algorithm based on an adaptive mutation scheme, weighted differential evolution algorithm (WDE), linear population size reduction success-history-based adaptive differential evolution algorithm, and biogeography-based optimization with covariance matrix-based migration] have been tackled for handling the current problem. The objective function is based on the cost of shallow foundation designs that satisfy ACI 318-05 requirements is formulated as the objective function. This study addresses shallow footing optimization with two attitudes, routine optimization, and sensitivity analysis. As a further study, the effect of the location of the column at the top of the foundation is examined by adding two additional design variables. Three numerical case studies are used for both routine and sensitivity analysis. Moreover, the most common evolutionary-based technique, genetic algorithm (GA), is considered as a benchmark to evaluate the proposed methods' efficiency. Based on the results, there is no algorithm which works as the most efficient solver over all the cases; while, BBO and WDE showed an acceptable performance because of satisfying records in most cases. There were several cases in which GA, DE, and ES were incapable of finding a valid solution which meets all the constraints simultaneously.

Keywords Metaheuristic algorithms · Global optimization · Construction industry · Shallow footing · Evolutionary algorithms

1 Introduction

In the past few decades, there has been an increasing demand for cost and performance optimality in structural design. However, finding the optimum design of a structure poses challenges due to material and design limit states prescribed in standard building codes. Therefore, developing a qualified design which meets both codes' requirements as well as optimality criteria simultaneously is a difficult task due to the high level of complexity and nonlinearity of engineering problems. Artificial intelligence as a perfect alternative has been helping engineers to deal successfully with a wide range of complicated problems (Akhani et al. 2019; Fister et al. 2014; Mousavi et al. 2015; Arab et al. 2018; Azizi et al. 2017; Derakhshan and Bashiri 2018; Ghoddousi et al. 2015; Rashki et al. 2019; Nikbakht and Papakonstantinou 2019).

Among a wide range of artificial intelligence-based techniques, metaheuristic optimization algorithms have been successfully applied to a wide-range of complicated problems in many different fields of reserach (Ide et al. 2016; Zeng et al. 2016; Mavrovouniotis et al. 2017; Hancer and Karaboga 2017; Zhou et al. 2016). Metaheuristic techniques search for sufficiently good solution rather than finding the global optimum. The fundamental mechanism of metaheuristic optimization algorithms may be based on two essential features: diversification and intensification. Diversification tries to diverge the search to explore the entire solution space, while intensification pushes the search towards the best-found solutions. The balance of these mechanisms influences the algorithms' performance

Communicated by V. Loia.

✉ Ali R. Kashani
kashani.alireza@ymail.com

[1] Department of Civil Engineering, University of Memphis, Memphis, TN 38152, USA

[2] Department of Civil Engineering, University of Tehran, Tehran, Iran

[3] School of Business, Stevens Institute of Technology, Hoboken, NJ 07030, USA

considerably. This characteristic is why metaheuristic algorithms show a different level of efficacy in dealing with a specific problem.

Recently, metaheuristic optimization algorithms have been widely used in construction industry-related problems, e.g., structural engineering (Gandomi et al. 2013; Yang et al. 2016; McCall and Balling 2017), water engineering, geotechnical engineering, transportation engineering (Yang et al. 2012; Celikoglu 2013; Omrani and Kattan 2013; Gandomi et al. 2015, 2017b, c; Kashani et al. 2016, 2019), construction management (Cheng et al. 2017; Lee et al. 2015), and structural damage detection (Kaveh 2017). Because of the stochastic nature of metaheuristic optimization algorithms and difference in performance of these techniques, they remain an active area of research (Elyasigomari et al. 2017; Meng and Pan 2017; Marinakis et al. 2017; Gandomi et al. 2015; Gandomi and Kashani 2016). As a result, it seems necessary to conduct the up-to-date research on the application of metaheuristic algorithms on a wide range of engineering problems.

Concrete structures are very important in the field of civil engineering; therefore, many researchers have worked on developing more sophisticated analyses and solution techniques to improve their design (Ghoddousi et al. 2016; Abbasnia et al. 2012, 2013; Khoshroo et al. 2018; Shayanfar et al. 2018; Rostamian et al. 2011; Omranian et al. 2018). However, structural designs that consider the operational and construction cost have not received the proper attention of engineering community. Spread foundation design and modeling is one of the most critical and sensitive concrete structural systems in geotechnical engineering. In fact, without a well-designed foundation to direct the effective loads to the earth successfully, most civil engineering structural systems cannot function. Therefore, the proper design of shallow footings is of vital importance to most construction projects. Since a considerable portion of a structure cost is associated with the foundations, cost-effective designs of footing are an essential concern for geotechnical engineers. With the development of metaheuristic algorithms, optimization of shallow footing has an very active area of research. Serviceability of footings is assessed by satisfying both geotechnical stability and structural strength. To account for both limit states in an shallow foundation optimization formulation, a variety of different design variables are required, as well as many nonlinear constraints. The resulting complexity of the objective function toward a level of complexity that can greatly affect the performance of optimization algorithms.

Although the research literature on different problems in civil engineering optimization is extensive (Camp and Akin 2011; Aydogdu 2017; Molina-Moreno et al. 2017; Gandomi et al. 2017a, b, c; Aydoğdu et al. 2016; Gholizadeh and Poorhoseini 2016; García-Segura et al. 2017; Tejani et al. 2018a, b, c, 2019; Kumar et al. 2018), there are relatively few studies on the optimum design of shallow footings. Wang and Kulhawy (2008) utilized a methodology to minimize the final cost of shallow footing based on the ultimate, limit, and serviceability state for low-cost design of a spread footing supporting a column under axial loading. In a similar study, Wang (2009) attempted to design a shallow footing based on a reliability-based optimization method. Khajehzadeh et al. (2011, 2012) enlisted a modified particle swarm optimization and gravitational search algorithm for designing of a shallow foundation. Khajehzadeh et al. (2013), developed a hybrid approach combines the firefly algorithm (FA) with the sequential quadratic programming (SQP), namely FaSqp, for the optimum design of shallow footings. Camp and Assadollahi (2013) took two different objectives, minimum cost and minimum CO_2 emission, into account for the design of footings under uniaxial loading case by applying a hybrid big bang-big crunch algorithm. Also, Camp and Assadollahi (2015) considered cost and CO_2 emission design of footing subjected to uniaxial uplift. Recently, Gandomi and Kashani (2018) considered the optimality of shallow footing by enlisting swarm intelligence algorithms [i.e., particle swarm optimization (PSO), accelerated particle swarm optimization (APSO), firefly algorithm (FA), levy-flight krill herd (LKH), whale optimization algorithm (WOA), ant lion optimizer (ALO), gray wolf optimizer (GWO), moth-flame optimization algorithm (MFO), and teaching–learning-based optimization algorithm (TLBO)].

This study examines the performance of three evolutionary-based techniques: differential evolution (DE), evolutionary strategy (ES), and biogeography-based optimization algorithm (BBO), for the optimum design of shallow footings. These algorithms are selected for this study due to their successful application to a wide range of complicated engineering problems. For example, Gandomi et al. (2017) utilized these algorithms for slope stability analysis and optimum design of retaining wall successfully. Many complex civil engineering optimization problems have been successfully solved using DE, ES, and BBO (Zhao et al. 2015; Seyedpoor et al. 2015; Franco et al. 2004; Jalili et al. 2016; Çarbaş 2017). In addition, this study considers the performance of several recently developed variations of DE, ES, and BBO algorithms [i.e., improved differential evolution algorithm based on an adaptive mutation scheme (IDE), weighted differential evolution algorithm (WDE), linear population size reduction success-history-based adaptive differential evolution algorithm (L-SHADE), and biogeography-based optimization with covariance matrix-based migration (CMM-BBO)]. Performance of these techniques is compared

benchmark genetic algorithm (GA) solutions. A MATLAB code is developed to analyze shallow footings based on ACI 318-05 (2005) requirements. The objective function considers as the total cost of a shallow footing and its construction. Two different loading cases of the uniaxial and flexural moment appied to the shallow foundation. In addition the effect of the column location on the footing surface is studied. Also, this study explores the sensitivity of different input parameters on the final design due to chances in the friction angle, the elasticity of modulus, Poisson's ratio, and density of the base soil, the depth of the footing and inclination of the effective load with respect to the vertical direction.

2 Methodology

Figure 1 shows a schematic of a shallow footing. Where L, B, and H represent the length, width, and thickness of footing, respectively, D is the depth of the bottom of footing from the ground surface, b_{col} is the column width, L_0 is the over-excavation length, and B_0 is the over-excavation width around the footing.

Geotechnical stability is measured by the factor of safety for bearing capacity FS_{B} given as:

$$FS_{\mathrm{B}} = \frac{q_{\mathrm{ult}}}{q_{\max}} \tag{1}$$

where q_{ult} is the ultimate bearing capacity of the soil, and $q_{\max}$ is the maximum allowable bearing pressure computed based on Meyerhof's (1963) general equation.

The second geotechnical requirement is based on settlement. In order to evaluate the elastic settlement of the footing, a method proposed by Algin (2009) is utilized as follows:

$$dS_a = \frac{1}{E_s}\int_0^H\int_0^L\int_0^B \left(-\frac{\{L(q_{\mathrm{b}}-q_{\mathrm{a}})x + B[Lq_{\mathrm{a}} + (q_{\mathrm{c}}-q_{\mathrm{a}})y]\}z(1+\mu_{\mathrm{s}})[2(x^2+y^2+z^2)\mu_{\mathrm{s}} - 3z^2]}{2\pi BL(x^2+y^2+z^2)^{5/2}}\right) d_x d_y d_z \tag{2}$$

where q_{a}, q_{b}, q_{c}, and q_{d} are the load intensities at the four consecutive corners of the foundation, μ_{s} is the Poisson's ratio for a given soil, and E_s is Soil elastic Young's modulus.

In addition to the geotechnical criteria, a number of structural requirements prescribed in ACI 318-05 (2005) must be considered in the final design.

The maximum and minimum soil pressure q_{u} under the footing due to vertical force and flexural moment are:

$$q_{\mathrm{u,max}} = \frac{P_{\mathrm{u}}}{BL} + \frac{6M_{\mathrm{u}}}{BL^2} \tag{3}$$

$$q_{\mathrm{u,min}} = \frac{P_{\mathrm{u}}}{BL} - \frac{6M_{\mathrm{u}}}{BL^2} \tag{4}$$

where P_{u} and M_{u} are the factored load and moment based on ACI 318-05 (2005).

The critical perimeter b_{perim} for two-way shear strength against punching of the column at $d_{\mathrm{ave}}/2$ away from each column face is

$$b_{\mathrm{perim}} = 4(b_{\mathrm{column}} + d_{\mathrm{ave}}) \tag{5}$$

Where b_{column} is the width of the column and d_{ave} is the average depth of compression fiber to the centroid of the reinforcement.

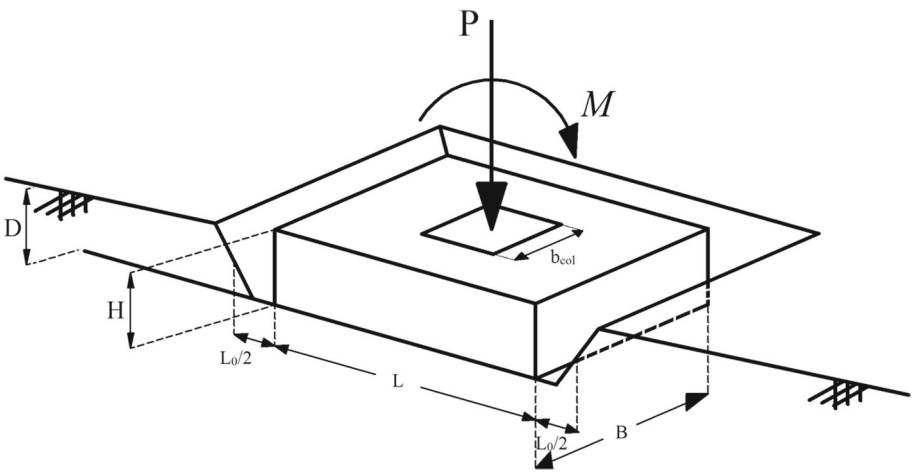

Fig. 1 Schematic view of a shallow footing

The critical two-way shear $V_{u,two\text{-}way}$ is calculated by

$$V_{u,two-way} = \frac{P_u}{b_{prim} \times d_{ave}} + \frac{\gamma_v M_{ux} b_{col}}{J_{cx}} + \frac{\gamma_v M_{uy} b_{col}}{J_{cy}} \quad (6)$$

where γ_v is a coefficient for determining shear portion from the unbalanced moment, M_{ux} and M_{uy} are the flexural moments in each direction, and J_{cx} and J_{cy} are the polar moments of inertia in each direction.

The nominal two-way shear strength $V_{n,\ two\text{-}way}$ is computed as

$$V_{n,two-way} = \phi \min \begin{cases} \frac{\sqrt{f'_c}}{3} b_{prim} \times d_{ave} \\ \left(1 + \frac{2}{\beta}\right) \frac{\sqrt{f'_c}}{6} b_{prim} \times d_{ave} \\ \left(\frac{\alpha_s d_{ave}}{b_{prim}} + 2\right) \frac{\sqrt{f'_c}}{6} b_{prim} \times d_{ave} \end{cases} \quad (7)$$

where β is the ratio of the long side to the short side of the column, ϕ is the nominal strength coefficient [ϕ = 0.75 as per ACI 318-05], α_s is a factor related to the column position on the footing, and f'_c is the compressive strength of the concrete.

The critical one-way shear, $V_{u,one\text{-}way}$ at a distance of d_{ave} away from the face of the column in each direction, is calculated as

$$V_{u,one-way,short} = qB\left(\frac{L}{2} - \frac{b_{col}}{2} - d_{ave}\right) \quad (8)$$

$$V_{u,one-way,long} = qL\left(\frac{B}{2} - \frac{b_{col}}{2} - d_{ave}\right) \quad (9)$$

One-way shear strength, $V_{n,one\text{-}way}$, is calculated as

$$V_{n,one-way} = \phi\left(0.17\omega d_{ave}\kappa\sqrt{f'_c}\right) \quad (10)$$

where κ is a factor representing the type of concrete and ω is B for the short and L for the long direction.

In addition to shear strength, the final design must withstand effective moments M_u on the critical sections located along the face of the column in each direction:

$$M_{u,short} = \frac{qB}{2}\left(\frac{L}{2} - \frac{b_{col}}{2}\right)^2 \quad (11)$$

$$M_{u,long} = \frac{qL}{2}\left(\frac{B}{2} - \frac{b_{col}}{2}\right)^2 \quad (12)$$

The flexural strength, M_n, is calculated in each direction as follows:

$$M_n = \phi A_{si} f_y \left(d_i - 0.59\frac{A_{si} f_y}{\omega f'_c}\right) \quad (13)$$

where A_{si} is the reinforcement cross-sectional area, f_y is the tensile strength of the reinforcing steel, and d_i is the depth from the compression face of the footing to the centroid of the reinforcement.

If ϕ states the reduction factor of bearing strength [equal to 0.65 based on ACI 318-05 (2005)], A_1 is the loading area (at the end of the column), and A_2 is the area of the lower base of the most substantial frustum of a pyramid with sides' inclination of 1–2 as shown in Fig. 2; the bearing strength of the concrete is given by Eq. (14).

$$P_{bearing,footing} = 0.85\phi f'_c A_1 \sqrt{\frac{A_2}{A_1}} \le 2 \times 0.85\phi f'_c A_1 \quad (14)$$

The bearing strength of the dowels $P_{bearing,\ dowel}$ is calculated as

$$P_{bearing,dowel} = \phi A_{s,dowel} f_y \quad (15)$$

Therefore, the total bearing strength $P_{bearing}$ may be calculated by:

$$P_{bearing} = P_{bearing,footing} + P_{bearing,dowel} \quad (16)$$

The next step is to determine the total length of reinforcement in the foundation. Therefore, computing the development length based on ACI 318-05 (2005) is necessary.

The minimum development length, l_d, for flexural elements is computed as

$$l_d = \frac{f_y \psi_s \psi_t \psi_e}{1.1\lambda\sqrt{f'_c}\left(\frac{c_b + K_{tr}}{d_{bar}}\right)} d_{bar} \quad (17)$$

where ψ_s is the size factor, ψ_t is the traditional reinforcement location factor, ψ_e is a coating factor reflecting the effects of epoxy coating, λ is a factor reflecting the lower tensile strength of lightweight concrete d_b is the diameter of the reinforcement, c_b, the smaller of the distance from the center of a bar to the nearest concrete surface and one-half the center-to-center spacing of the bars being developed, and K_{tr} represents the contribution of confining reinforcement across potential splitting planes and is taken as zero. In this study, ψ_t, ψ_e, and λ are 1.0 and ψ_s is 0.8 for #6 bars and smaller bars and 1.0 for bars larger than #6.

If d_{dowel} is the diameter of the dowels, the development length of the dowels into the column, $l_{d,dowel,col}$, is computed as

$$l_{d,dowel,col} = \max(0.0005 f_y d_{dowel}, l_{d,col}) \quad (18)$$

where d_{dowel} is the diameter of the dowels and $l_{d,\ col}$ is the development length of the column reinforcement is

$$l_{d,col} = \max\left(\frac{0.24 d_{col} f_y}{\sqrt{f'_c}}, 0.043 d_{col} f_y, 200\,\text{mm}\right) \quad (19)$$

where d_{col} is the diameter of the column bars.

The development of the dowel into the footing $l_{d,\ the\ dowel}$ is

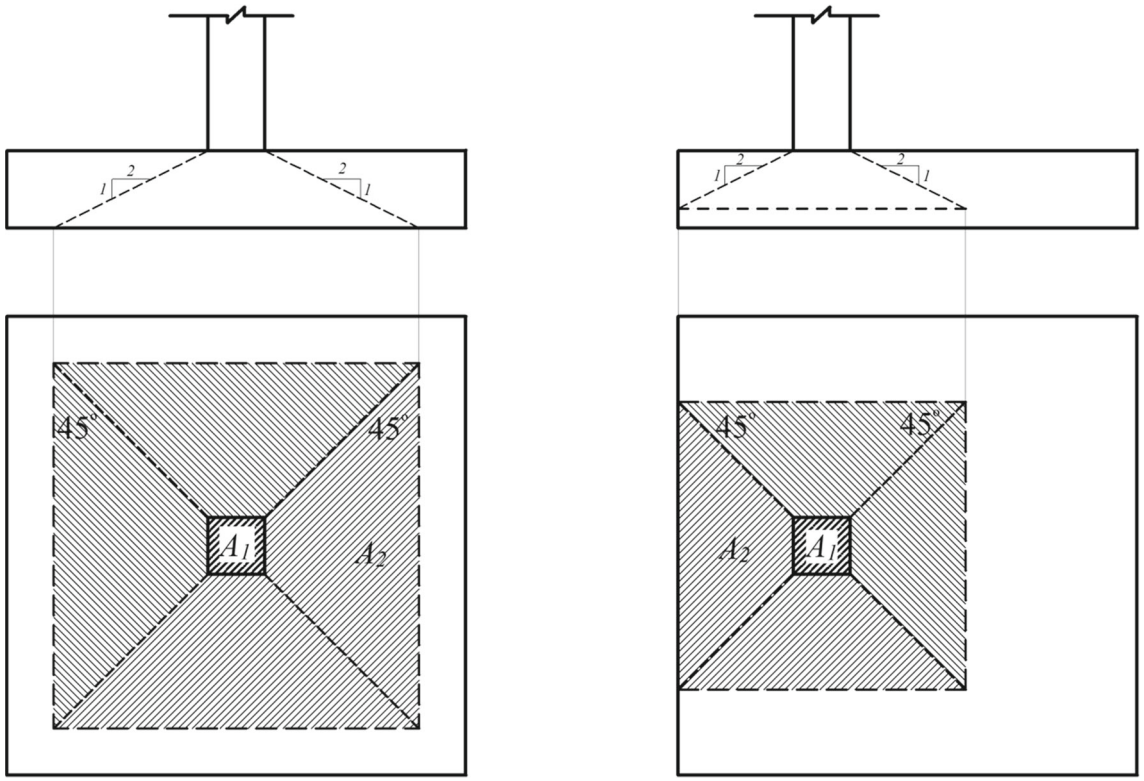

Fig. 2 The position of A_1 and A_2 for computing bearing strength of the concrete

$$l_{\mathrm{d,col}} = \max\left(\frac{0.24 d_{\mathrm{dowel}} f_{\mathrm{y}}}{\sqrt{f'_{\mathrm{c}}}}, 0.043 d_{\mathrm{dowel}} f_{\mathrm{y}}, 200\ \mathrm{mm}\right) \quad (20)$$

All the above-mentioned limitations control either geotechnical or structural constraints. Table 1 lists the inequality constraint formulations for the design of shallow foundation. where δ is the settlement, V is the shear strength, M is the flexural strength, A_{si} is the reinforcement area, ε_{s} is the tension steel strain, $l_{\mathrm{d,\ short}}$ is the development length in short direction, $l_{\mathrm{d,\ long}}$ is the development length in long direction, $s_{\min}$ is the minimum spacing of reinforcement, $s_{\max}$ is the maximum spacing of reinforcement, P_{u} is the maximum bearing pressure, $D_{\max}$ is the maximum depth of footing, $D_{\min}$ is the minimum depth of footing, and *cover* is the concrete cover. E_{x} and E_{y} in Table 1 are distance of the column from the center parallel to X and Y direction.

3 The objective function for optimization

Figure 3 defines nine design variables for the design of a shallow foundation: the length (X_1), the width (X_2), the thickness (X_3), the depth of footing (X_4), the bar number in the long direction (R_1), the number of bars in the long direction (R_2), the bar number in short direction (R_3), the number of bars in short direction (R_4), and bar number of the dowels (R_5). In addition, two design variables, E_x and E_y, defined the location of the column on the top of the foundation.

The objective function for the minimum cost design of shallow footing is

$$f_{\mathrm{cost}} = C_{\mathrm{e}} V_{\mathrm{e}} + C_{\mathrm{f}} A_{\mathrm{f}} + \xi C_{\mathrm{r}} M_{\mathrm{r}} + \frac{f'_{\mathrm{c}}}{f'_{\mathrm{cmin}}} C_{\mathrm{c}} V_{\mathrm{c}} + C_{\mathrm{b}} V_{\mathrm{b}} \quad (21)$$

where C_{e} is the unit cost of excavation, C_{f} is the unit cost of the framework, C_{r} is the unit cost of reinforcement, C_{c} is the unit cost of concrete, C_{b} is the unit cost of backfill, V_{c} is the concrete volume, and V_{b} is backfill volume, respectively. Table 2 lists relevant unit cost values.

To handle the mentioned constraints, a static penalty function approach proposed by Homaifar et al. (1994) is utilized. In this way, the objective function would be imposed by a penalty value that reflects the degree of constraint violations.

$$\mathrm{fitness}_i(X) = f_i(X) + \sum_{j=1}^{m} R_{k,j} \phi_j^2(X) \quad (22)$$

where $R_{i,j}$ are the penalty coefficients used, ϕ_j is the amount of violation, m is the number of constraints, $f(X)$ is

Table 1 Inequality constraints

Constraint	Function
$g_1(x)$	$\frac{\mathrm{FS}_{\mathrm{Bdesign}}}{\mathrm{FS}_{\mathrm{B}}} - 1 \leq 0$
$g_2(x)$	$\frac{\delta}{\delta_{\max}} - 1 \leq 0$
$g_{[3-5]}(x)$	$\frac{V_u}{V_n} - 1 \leq 0$
$g_{[6-7]}(x)$	$\frac{M_u}{M_n} - 1 \leq 0$
$g_{[8-10]}(x)$	$\frac{A_{s\min}}{A_s} - 1 \leq 0$
$g_{[11-12]}(x)$	$\frac{\varepsilon_s}{0.005} - 1 \leq 0$
$g_{13}(x)$	$\frac{l_{\mathrm{d,short}}}{\frac{B}{2} - \frac{b_{\mathrm{col}}}{2} - \mathrm{cover}} - 1 \leq 0$
$g_{14}(x)$	$\frac{l_{\mathrm{d,long}}}{\frac{L}{2} - \frac{b_{\mathrm{col}}}{2} - \mathrm{cover}} - 1 \leq 0$
$g_{15}(x)$	$\frac{2\mathrm{cover} + d_{\mathrm{b,long}} + d_{\mathrm{b,short}} + d_{\mathrm{dowel}} + l_{\mathrm{d,dowel}} + d_{\mathrm{bend}}/2}{H} - 1 \leq 0$
$g_{[16-17]}(x)$	$\frac{2\mathrm{cover} + n_{\mathrm{bars}} d_b + (n_{\mathrm{bars}} - 1) s_{\min}}{\omega} - 1 \leq 0$
$g_{[18-19]}(x)$	$\frac{\omega}{2\mathrm{cover} + n_{\mathrm{bars}} d_b + (n_{\mathrm{bars}} - 1) s_{\max}} - 1 \leq 0$
$g_{20}(x)$	$\frac{P_u}{P_{\mathrm{bearing}}} - 1 \leq 0$
$g_{21}(x)$	$\frac{D}{D_{\max}} - 1 \leq 0$
$g_{22}(x)$	$\frac{D_{\min}}{D} - 1 \leq 0$
$g_{23}(x)$	$\frac{\lvert E_x \rvert}{\frac{L}{2}} - 1 \leq 0$
$g_{24}(x)$	$\frac{\lvert E_y \rvert}{\frac{B}{2}} - 1 \leq 0$

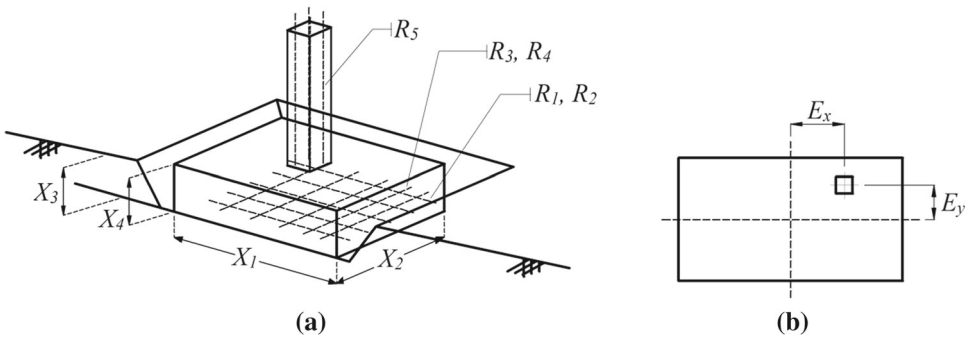

Fig. 3 Design variables for describing the shallow footing

Table 2 Unit cost values

Input parameter	Unit	Symbol	Value
Excavation	$/m^3	C_e	25.16
Concrete framework	$/m^2	C_f	51.97
Reinforcement	$/kg	C_r	2.16
Concrete	$/m^3	C_c	173.96
Compacted backfill	$/m^3	C_b	3.97

the unpenalized objective function, and $k = 1, 2, \ldots, l$, where l is the number of levels of a violation defined by the user.

4 Optimization algorithms description

4.1 Genetic algorithm

The genetic algorithm (GA) is an evolutionary algorithm imitating biological rules developed by Holland (1975). In a GA, each potential solution to an optimization problem is called an individual and is composed of a series of genes called chromosome. In this chromosome, each gene represents one of the design variables. Therefore, each individual indicates a possible solution for a given function. A population of individuals surveys the search space generation to generation based on the fundamental theory of evolution. The fitness of every individual is attributed to the value of the objective function for the optimization problem. New generations reproduced iteratively via three

evolutionary operators: reproduction, crossover, and mutation. First, the highest ranked individuals would emerge in the next generation without a change in their content. Next, a group of fittest solutions works as parents to make offsprings. To this end, the crossover operator combines genes and proposes new chromosomes. Children will be modified slightly following a random pattern using a mutation operator. The mutation changes a gene in a chromosome based on a predefined probability. These GA operators are applied iteratively to successive populations until a satisfactory results is reached for termination. The GA in this study uses single-point crossover with a probability of 1, a mutation probability of 0.01, and a roulette wheel selection operator was for reproduction.

4.2 Differential evolution

4.2.1 Original differential evolution

Differential evolution (DE) is a population-based evolutionary algorithm developed by Storn and Price (1997). Similar to GA, DE starts evolving an initial random population using three basic evolutionary operators: selection, mutation, and crossover applied from generation to generation. The main difference between GA and DE is encoding that parameters using a float coding instead of a binary one. DE considers a mutation based on distance and direction information from the current population (Pant et al. 2008). The mentioned mutation operator adds a factored difference between two individuals (difference vector) to the third one (target vector) to reproduce new solutions called the trial vector. The mutation operator for the new solution S_i can be formulated as

$$S_i = S_j + F(S_k - S_l) \tag{23}$$

where S_j, S_k, and S_l be three randomly selected solutions from the current generation where j, k, and $l \epsilon \{1, 2, 3, \ldots, N\}$, and N is the population size, and F is a weighting factor.

In the next step, a crossover operator will be applied to the mutated solution with a probability of $C_r \epsilon [0, 1]$ as follows:

$$P_{i,t} = \begin{cases} S_{i,t} & \text{if } r(t) \le C_r \text{ or } t = rn(i) \\ S_{j,t} & \text{if } r(t) > C_r \text{ and } t \ne rn(i) \end{cases} \tag{24}$$

where $i = \{1, 2, 3, \ldots, D\}$ represent the tth variable of each individual (with D total variables), $r(t)$ is a uniform random number within [0, 1], and $rn(i)$ is a randomly chosen index, $rn(i) = \{1, 2, 3, \ldots, D\}$, that warrants getting at least one variable from S_i.

The aforementioned steps will be repeated iteratively until reaching termination criteria. In this study, the weighting factor is equal to 0.5, and the crossover rate is 0.5.

4.2.2 Improved differential evolution algorithm based on an adaptive mutation scheme

Ho-Huu et al. (2016) developed an improved differential evolution (IDE) based on an adaptive mutation scheme. IDE is different from the original DE in terms of selection and mutation operators. Padhye et al. (2013) proposed an elitist selection strategy in IDE. In this way, both the parents and children populations are considered altogether, and the best solutions among all of them would be selected as the next generation.

Second, the mutation in original DE was replaced by an adaptive multi-mutation scheme. In this way, within each generation, two of the following four popular mutation schemes including "rand/1," "best/1," "rand/2," and "best/2" were chosen following an adaptive procedure to trigger the mutation. This adaptive strategy pushed the algorithm to use "rand/1" and "rand/2" mutation schemes with more probability in the initial iterations to provide exploration while "best/1" and "best/2" mutation schemes are more probable in later iterations. This adaptive technique compares a determinant time-dependent parameter called delta with a predefined threshold to choose between the above mentioned cases. The time-dependent delta is computed as:

$$\text{delta} = \left| f_{\text{mean}} / f_{\text{best}} - 1 \right| \tag{25}$$

where f_{best} is the objective function value of the best individual and f_{mean} is the mean objective function value of the whole population.

4.2.3 Weighted differential evolution algorithm

The weighted differential evolution algorithm (WDE) is a recent variation of differential evolution algorithm proposed by Civicioglu et al. (2018). In this algorithm, a novel mutation operator is defined, which works with two population sets at every iteration. The fundamental steps of WDE are summarized as follows:

First, consider the population size to be N, at each iteration WDE deals with a set of $2 \times N$ solution vectors. First, a sub-pattern matrix called *SubP* will be constructed by N randomly selected vectors from the whole $2 \times N$ pattern vectors. Next, a temporary vector called *TempP* with the size of N will be generated using the rest of unselected solution vectors in the previous step (P_{rest}) by the following equation:

$$TempP = \sum (w \circ P_{\text{rest}}) \text{ where } \begin{cases} w = \dfrac{w_i^*}{\sum_v^N w_i^*} \times \Delta \\ w^* = \kappa^3_{(N \times 1)} \end{cases} \tag{26}$$

where ∘ represents an element-by-element multiplication, Δ is a 1-by-D vector whose elements are equal to one, and $\kappa_{(N\times 1)}$ is a N-by-1 vector of random numbers.

In WDE, a control parameter of $M_{(1:N,1:D)} = 0$ is defined which will be updated in the course of iterations based on the following equation:

$$M_{(indexJ)}: = 1 \text{ where } \begin{cases} J = V(1:\lceil K \times D \rceil) \\ V = permute(j0) \end{cases} \tag{27}$$

where K would is calculated as

$$\text{If } \alpha < \beta \text{ then } K = \kappa^3_{(1)} \text{ else } \quad K = \left(1 | -\kappa^3_{(1)}\right) \tag{28}$$

where α, β, and κ are uniform random numbers between 0 and 1, and the presented subscribes of κ (i.e., (.)) defines the size of this vector.

In WDE, a scale factor of F is defined as

$$\begin{cases} F_{(1\times D)} = \lambda^3_{(D)} & \text{If } \alpha' < \beta' \\ F_{(N\times D)} = \lambda^3_{(N)} \times \Delta & \text{Otherwise} \end{cases} \tag{29}$$

where λ is a vector of uniform random number within 0 and 1. The provided subscribes for the mentioned parameters show the dimension of the vectors.

Finally, the offspring will be generated as follows

$$\begin{cases} T = SubP + F \times M \circ \left(TempP - SubP_{(m)}\right) \\ m = permute(i) | m \neq [1:N] \end{cases} \tag{30}$$

here, $i = 1{:}\ N$ where $i \in Z^+$.

If the value of a design variable falls outside the domain, the value are reset using

$$\begin{cases} P_i = \text{lb}_i + \kappa^3_{(1)} \times (\text{ub}_i - \text{lb}_i) & \text{if } P_i < \text{lb}_i \\ P_i = \text{ub}_i + \kappa^3_{(1)} \times (\text{lb}_i - \text{ub}_i) & \text{if } P_i > \text{ub}_i \end{cases} \tag{31}$$

where $\kappa(1)$ is a uniform random number with the size of 1, and lb_i and ub_i are lower and upper bounds, respectively.

4.2.4 Linear population size reduction success-history-based adaptive differential evolution algorithm

Tanabe and Fukunaga (2014) proposed L-SHADE as an enhanced version of the success-history-based adaptive differential evolution algorithm (SHADE) by considering linear population size reduction (LPSR). In fact, SHADE is an improved version of a well-known, DE variant which employs a control parameter adaptation mechanism called JADE (Zhang and Sanderson 2009). In this section, a short description is provided for common features of JADE, SHADE, and L-SHADE, and additional modifications utilized in L-SHADE.

The first common feature between the three mentioned algorithms is utilizing a generalized form of "current-to-best/1" mutation strategy called "current-to-best/1." This mutation strategy presented in Eq. (32) uses one of the randomly selected individuals from top $N \times p$ ($p \in [0, 1]$) members of G-th generation ($x_{pbest,G}$) instead of using the global best solution.

$$v_{i,G} = x_{i,G} + F_i \cdot (x_{pbest,G} - x_{i,G}) + F_i \cdot (x_{r1,G} - x_{r2,G}) \tag{32}$$

where the parameter $F_i \in [0, 1]$ controls the magnitude of the differential mutation operator used by individual x_i. $x_{r2,G}$ in Eq. (31) will be selected randomly from the union of parents and archived solutions. In this mutation strategy, the control parameter p is defined to adjust greediness and provide a balance between exploration and exploitation.

The second feature is enlisting an external archive in which the unselected parents are saved. The size of archive memory is equal to the population size.

The third feature are the control parameters assignments utilized in SHADE and L-SHADE which are different from the JADE algorithm. To be more exact, a historical memory with the size of H is provided to SHADE and L-SHADE for two control parameters (i.e., C_r and F) in DE. Both these parameters C_r and F vary between 0 and 1 which are crossover rate and scaling factor for magnitude of mutation, respectively. An effective approach was utilized in SHADE is to update this memory in each generation with C_{ri} and F_i values, which result in better offsprings (Tanabe and Fukunaga 2014).

Finally, LPSR has been incorporated into SHADE algorithm for dynamically resizing the population size to improve its performance. To this end, in each iteration, the following equation is proposed to examine the population size for the next generation:

$$N_{G+1} = round\left[\left(\frac{N^{\min} - N^{\text{init}}}{MAX\_NFE}\right) \cdot NFE + N^{\text{init}}\right] \tag{33}$$

where $N^{\min}$ is the minimum possible number of the individuals for mutation (proposed to be equal to 4), N^{init} is initial population size, NFE is the current number of fitness evaluations, and MAX_NFE is the maximum number of fitness evaluations. Therefore, in each generation ($N_G - N_{G+1}$), numbers of the worst individuals would be removed from the population.

4.3 Evolutionary strategy

Evolution Strategy (ES) was originally proposed by Rechenberg (1965), and later developed by Schwefel (1977). ES mimics macro-level of evolution (phenotype, hereditary, variation) to explore the solution space (Brownlee 2011). The major difference between GA and ES is using a string of real number to represent the potential solutions rather than a bit string. ES works mainly based on three key steps:

(i) producing new offspring from a set of parents using a recombination operator
(ii) applying a mutation operator to provide exploitation
(iii) generating a new population by collecting the fittest group of solutions

This study utilizes a two-member ES, which forms new offspring P from the parent S_p based on

$$P = S_p + Z \tag{34}$$

where $Z = \{z_1, z_2, z_3, \ldots, z_n\}$ is a random vector of a size consistent with the problem's dimensions.

Moreover, the following probability function is proposed for the mutation operator:

$$p(z_i) = \frac{1}{\sqrt{(2\pi)\sigma_i}} \exp\left(-\frac{(z_i - \xi_i)^2}{2\sigma_i^2}\right) \tag{35}$$

where z_i is the ith component and ξ_i and σ_i are the mean and standard deviation of z_i, respectively.

ES applies these steps iteratively to reach a solution to the optimization problem. In this study the the number of offspring to produce each generation is set at 10 and the standard deviation for changing the solution is set as 1.

4.4 Biogeography-based optimization algorithm

4.4.1 The original biogeography-based optimization algorithm

The biogeography-based optimization (BBO) algorithm is inspired by mathematical models of biogeography proposed by Simon (2008). Biogeography is a study of the distribution of different biological species among islands over time by Wallace (1876) and Darwin (1859). In BBO, each island is represented by a potential solution. Those habitats move toward the fitter solution by frequent updates via migration and mutation operators. BBO controls the search direction toward the optimal solution by defining two parameters that govern the sharing of features between solutions. These parameters λ and μ are defined as

$$\lambda_s = I\left(1 - \frac{S}{S_{max}}\right), \quad \text{for } 0 \le S \le S_{max} \tag{36}$$

$$\mu_s = E\frac{S}{S_{max}}, \quad \text{for } 0 \le S \le S_{max} \tag{37}$$

where S_{max} is the most significant possible number of species, S is the number of species, I is the maximum immigration rate, and E is the maximum emigration rate.

An island's potential to absorb habitants is defined by a suitability index variable (SIV). Larger values of the SIV illustrate the more capacity for accepting more individuals. However, the quality of individuals was examined by habitat suitability index (HSI).

In a BBO algorithm, a weak solution with higher potential of change will accept new immigrants from a better solution (higher HSI). Therefore, poor solutions experience more alterations to improve their positions. Moreover, a mutation operator provides a satisfactory diversity of the solutions in BBO. This study used a mutation probability of 0.01, and habitat modification probability of 1.

4.4.2 Biogeography-based optimization with covariance matrix-based migration

Chen et al. (2016) proposed a modified version of the original BBO algorithm by incorporating covariance-based matrix migration (CMM-BBO) which eliminates the dependence of original BBO to the coordinate system.

Basically, CMM rotates the coordinate system by applying an eigenvector to a given solution vector (H) before the migration procedure in order to provide more efficient information transition.

Eigenvectors can be evaluated using a factorized covariance matrix of the solution vector with the size of D as follows:

$$\mathrm{Cov}(H) = Q_H \Lambda_H Q_H^T \tag{38}$$

where Q_H is the $D \times D$ matrix that has the eigenvector of $\mathrm{Cov}(H)$ as its ith column and Λ_H is the diagonal matrix that has the corresponding eigenvalues as its diagonal entries, respectively.

The eigenvector-based solution will be generated using a factorized covariance matrix $\mathrm{Cov}(H)$ into its canonical form based on

$$\begin{cases} eigH_k^G = H_k^G \times Q_H \\ eigH_k^G = [eigH_{(k,1)}^G, eigH_{(k,2)}^G, \ldots, eigH_{(k,D)}^G] \end{cases} \tag{39}$$

where G represents the current generation, $eigH_k^G$ denotes the rotated habitant, and $eigH_{(k,j)}^G$ is the jth rotated SIV in the eigenvector-based coordinate system. In this study, the crossover rate and probability of using covariance matrix-based migration are 0.9 and 0.5, respectively.

5 Numerical simulation

Three numerical case studies are examined to estimate the performance of the proposed algorithms. The first case addresses a shallow footing which subjected to a uniaxial load. In the second case, an effective moment is added to the uniaxial force. The third case considers the impact of relocating the column along the top of the footing in each

Table 3 Utilized data for case studies

Input parameters	Unit	Symbol	Routine optimization	Sensitivity analysis
Internal friction angle of base soil	°	ϕ	30	30
Unit weight of base soil	kN/m^3	γ_s	18	19.5
Poisson's ration	–	μ_s	0.3	0.5
Elasticity modulus of soil	kPa	E_s	10,500	30,500
Over-excavation length	m	L_0	0.3	0.3
Over-excavation width	m	B_0	0.3	0.3
Yield strength of reinforcing steel	MPa	f_y	400	400
Compressive strength of concrete	MPa	f_c	21	21
Concrete cover	cm	C_c	7	7
Unit weight of concrete	kN/m^3	γ_c	23.5	23.5
Depth of bottom of the footing from the ground surface	m	D	0.5	0.5
Maximum allowable settlement	mm	δ	25	25
The factor of safety for bearing capacity	–	$SF_{B,design}$	3	3

direction. Table 3 lists the necessary input parameters for the case studies. MATLAB is used to develop a design procedure for determining the minimum cost design of shallow footing based on ACI 318-05 requirements. To compute meaningful statistics on the performance of the proposed algorithms all each algorithm is run run 101 times. The results are reported based on best, worst, mean, median, and standard deviation (SD) of the runs. For all algorithms, the population size is 50 and maximum number of iterations is 1000. As a further study, a sensitivity analysis is conducted on variations of soil parameters base soil friction angle variation between 28° and 38°, soil density between 11.5 and 23.5 kN/m^3, modulus of elasticity between 10,500 and 90,500 kPa, Poisson's ratio between 0.1 and 1, concrete compressive strength between 20 and 55 MPa, effective force inclination with respect to vertical axis between 0° and 45°, and depth of footing between 300 and 3000 mm. The column for conveying the loading to the footing has an area of 400 × 400 mm^2 with reinforcements' composition of 6Φ16. Table 4 lists the limits for each design variable.

5.1 Case I: uniaxial loading

In this case, the shallow footing is subjected to a uniaxial force yield developed from dead and live loads of 650 kN and 350 kN, respectively. In a series of 101 runs, GA, DE, and ES were successful in reaching a valid solution 51, 57, and 62 times. Table 5 lists data gathered on the cost of the final designs in the form of the best, worst, mean, SD, and median values based on the number of cases that algorithms worked efficiently in finding valid solutions. Table 6 lists the final design variables. These results show that L-SHADE and IDE generated the lowest cost design at $29,884.24. Furthermore, L-SHADE was the best algorithm in this case of study based on values for worst, mean, SD and median of $43,442.27, $36,140.85, $3000.00, and $36,163.22, respectively. On the other hand, the highest best value is obtained by GA. Also, based on the mean values, ES showed the poorest performance with a mean value of $119,866.19.

Table 7 lists values for each component related to the objective function. Using L-SHADE results as the benchmark, excavation is reduced by 30.92%, 41.06%, 62.42%, and 20.74% with respect to GA, DE, ES, and WDE, respectively. Concrete framework was reduced by 11.45%, 24.65%, 31.44%, and 0.79%, reinforcement reduced by 54.52%, 37.61%, 47.89%, and 0%, concrete volume reduced by 20.32%, 37.13%, 48.97%, and 0.67%, and compacted backfill reduced by 24.88%, 32.08%, 52.48%, and 20.49% in comparison with GA, DE, ES, and WDE, respectively. Comparing the results between L-SHADE and BBO demonstrates 2.97% less excavation and 12.41% less compacted backfill proposed by BBO, while 10.61% more solid framework, 16.56% more reinforcement, and 19.89% more concrete obtained by BBO.

Table 8 list design results for this case from previous studies. The results from most of the proposed methods show better performance in terms of except best, mean, SD, and median solution except for GA, DE, and ES.

Figure 4(a) shows convergence rate plots for the best-found solutions. These plots indicate that the GA, DE, and ES methods were considerably less efficient than the other methods and did not successful converge to a valid solution in the initial iterations (e.g., GA found a valid solution after the 79th iteration, DE after 421st iteration, and ES after 856th iteration). These algorithms followed an invariant pattern until converging to the final solutions. Figure 4(a) shows that BBO, L-SHADE, and IDE converged to their best-found solution relativity quickly WDE

Table 4 Design variables permitted domains

Design variables	Unit	Lower bound	Upper bound
X_1	cm	400	4000
X_2	cm	400	4000
X_3	cm	0	3000
X_4	cm	300	3000
R_1	–	2	20
R_2	–	3	18
R_3	–	2	20
R_4	–	3	18
R_5	–	4	20
E_x	cm	− 2000	2000
E_y	cm	− 2000	2000

recorded lots of changes and improvements during the search. Figure 4(b) shows mean convergence history for all the algorithms. For this case study, these plots indicted that L-SHADE and CMM-BBO have satisfactory performance, while BBO, IDE, and WDE were inefficient, and GA, DE, and ES displayed the weakest performance.

5.2 Case II: axial and flexural loading at the center of foundation

In this case, the foundation is subjected to an external moment from the dead and live load as 400 kN m and 150 kN m in addition to the vertical forces defined in the Case I. Table 5 lists the best, worst, mean, SD, and median values for Case II low-cost design from 101 runs. Only BBO and WDE were are to find feasible low cost designs. While the best design was obtained by BBO, WDE demonstrated overall better performance in this case study. To be more precise, the best-found solution by WDE is only 0.07% more than BBO while its worst, mean, SD, and median were 60.74%, 10.37%, 95.98%, and 1.01% less than BBO. Moreover, WDE was successful in converging to a feasible solution 101 times while BBO was successful only 60 times.Tables 6 and 9 list the design variables and operational expenses, respectively. These data also

Table 5 Design cost values for numerical case studies

Optimization algorithm	Best	Worst	Mean	SD	Median	Successful run
Case I						
GA	65,202.98	214,203.5	108,384.9	30,889.48	100,168	51
DE	47,854.12	234,763.3	115,026.2	40,560.58	107,810.6	57
ES	57,491.74	201,798.9	119,866.2	38,165.27	109,785.5	62
BBO	35,729.92	711,79.83	45,976.71	5496.31	44,713.83	101
L-SHADE	29,884.24	43,442.27	36,140.85	3000.00	36,163.22	101
CMM-BBO	32,593.32	43,442.27	36,306.05	1857.04	36,163.22	101
IDE	29,884.24	86,792.60	40,803.87	6936.81	39,251.28	101
WDE	29,975.51	40,982.80	37,171.43	2419.07	37,774.61	101
Case II						
GA	N.G.	N.G.	N.G.	N.G.	N.G.	0
DE	N.G.	N.G.	N.G.	N.G.	N.G.	0
ES	N.G.	N.G.	N.G.	N.G.	N.G.	0
BBO	82,586.08	223,702.4	95,031.69	25,601.23	86,057.1	60
L-SHADE	N.G.	N.G.	N.G.	N.G.	N.G.	0
CMM-BBO	N.G.	N.G.	N.G.	N.G.	N.G.	N.G.
IDE	N.G.	N.G.	N.G.	N.G.	N.G.	N.G.
WDE	82,641.39	87,822.48	85,174.01	1029.10	85,184.41	101
Case III						
GA	N.G.	N.G.	N.G.	N.G.	N.G.	N.G.
DE	N.G.	N.G.	N.G.	N.G.	N.G.	N.G.
ES	N.G.	N.G.	N.G.	N.G.	N.G.	N.G.
BBO	49,432.67	406,799.4	68,315.1	35,051.68	63,301.79	101
L-SHADE	N.G.	N.G.	N.G.	N.G.	N.G.	0
CMM-BBO	N.G.	N.G.	N.G.	N.G.	N.G.	N.G.
IDE	N.G.	N.G.	N.G.	N.G.	N.G.	N.G.
WDE	54,271.58	71,325.71	62,659.25	4314.35	62,688.27	36

Table 6 Final low-cost optimization designs for the proposed case studies

Optimization algorithms	X_1 (m)	X_2 (m)	X_3 (m)	X_4 (m)	R_1	R_2	R_3	R_4	R_5	E_x	E_y
Case I											
GA	1355.02	1351.58	1902.34	310.94	14	17	16	11	14	–	–
DE	1635.16	1366.55	1947.95	361.28	14	14	14	16	18	–	–
ES	1642.17	1806.07	2511.80	350.66	14	17	16	12	18	–	–
BBO	1361.95	1362	1265.77	301.41	14	13	12	17	14	–	–
L-SHADE	1180.38	1180.38	1567.86	300	12	16	12	16	14	–	–
CMM-BBO	1180.38	1352.11	1393.212	300	12	17	14	12	14	–	–
IDE	1180.38	1180.38	1567.861	300	12	16	12	16	14	–	–
WDE	1181.16	1185.14	1969.71	302.80	12	16	12	16	14	–	–
Case II											
GA	–	–	–	–	–	–	–	–	–	–	–
DE	–	–	–	–	–	–	–	–	–	–	–
ES	–	–	–	–	–	–	–	–	–	–	–
BBO	1696	2901	1037	336.38	18	16	16	12	14	–	–
L-SHADE	–	–	–	–	–	–	–	–	–	–	–
CMM-BBO	–	–	–	–	–	–	–	–	–	–	–
IDE	–	–	–	–	–	–	–	–	–	–	–
WDE	1696.05	2901.69	1240.77	336.52	18	16	16	12	14	–	–
Case III											
GA	–	–	–	–	–	–	–	–	–	–	–
DE	–	–	–	–	–	–	–	–	–	–	–
ES	–	–	–	–	–	–	–	–	–	–	–
BBO	1654	1712.93	1927.76	301.11	14	15	14	15	14	− 4	− 180
L-SHADE	–	–	–	–	–	–	–	–	–	–	–
CMM-BBO	–	–	–	–	–	–	–	–	–	–	–
IDE	–	–	–	–	–	–	–	–	–	–	–
WDE	1624.29	1796.59	1988.56	344.47	16	13	14	16	14	41.80	221.60

Table 7 Level of construction operations and facilities for Case I

The resultant operations content	Unit	Value							
		GA	DE	ES	BBO	L-SHADE	CMM-BBO	IDE	WDE
Excavation	m^3	8.02	9.40	14.74	5.38	5.54	5.38	5.54	6.99
Concrete framework	m^2	4.28	5.03	5.5284	4.24	3.79	4.00	3.79	3.82
Reinforcement	kg	2.99 E+03	2.18E+03	2.61E+03	1.63E+03	1.36E+03	1.48E+03	1.36E+03	1.36E+03
Concrete	m^3	1.87	2.37	2.92	1.86	1.49	1.66	1.49	1.50
Compacted backfill	m^3	2.17	2.40	3.43	1.45	1.63	1.52	1.63	2.05

confirms that GA, DE, ES, IDE, and WDE failed to converge to a fesiable final design.

Tables 10, 11, 12, 13, 14, 15, and 16 list the results of a sensitivity analysis of the effect of various soil parameters to the final design based on the best and mean results of 101 runs. Figures 5, 6, and 7 shows a comparison of mean values for each optimization method for variations in the values of soil parameters. It worth noting that the results are based on the successful runs from the original 101 runs. The results in Table 10 show considerable change in the low-cost designs as D_f varies from 300 mm to 3000 mm. BBO and WDE both solved the problem efficiently, while the performance of other algorithms was varied sporadically. The results demonstrated that increasing the depth of

Table 8 Design cost values for numerical case studies recorded in the previous studies (Gandomi and Kashani 2018)

Optimization algorithm	Best	Worst	Mean	SD	Median
Case I					
PSO	43,442.27	174,424.19	68,735.94	25,816.84	65,635.62
APSO	43,443.57	101,988.36	59,688.07	13,129.36	56,338.39
FA	43,460.08	56,392.56	47,889.69	4050.38	48,655.36
LKH	43,442.27	121,053.07	60,307.73	20,401.16	50,854.70
WOA	44,069.07	269,536.09	74,438.94	33,273.80	63,619.03
ALO	43,449.55	86,639	54,489.32	9100.66	51,528.52
GWO	43,449.51	50,867.28	44,099.64	1896.90	43,548.68
MFO	43,442.27	92,818.80	52,244.01	11,878.01	47,177.09
TLBO	43,442.27	80,530.39	50,030.90	6983.25	48,867.28
Case II					
PSO	N.G.	N.G.	N.G.	N.G.	N.G.
APSO	83,106.50	199,333.61	111,235.31	39,132.04	88,429.40
FA	83,420.23	95,344.62	87,260.74	2048.08	86,752.26
LKH	82,561.80	168,203.28	103,150.55	31,489.16	84,684.55
WOA	86,211.90	213,337.85	143,928.04	28,789.61	141,308.61
ALO	82,591.50	171,792.51	91,960.91	11,750.99	87,682.61
GWO	82,913.69	86,744.27	84,424.89	905.71	84,722.97
MFO	82,561.80	193,416.99	98,280.99	17,005.85	89,082.68
TLBO	82,561.80	91,131.93	84,042.91	1319.29	83,357.92
Case III					
PSO	50,774.31	133,384.03	60,345.81	14,491.96	56,501.26
APSO	50,477.45	153,021.38	65,808.17	14,359.98	61,379.86
FA	50,582.63	71,602.48	59,828.52	3806.46	59,357.75
LKH	48,720.24	625,896.24	75,764.29	60,913.08	63,923.62
WOA	62,785.04	726,015.73	147,202.86	96,514.92	121,278.82
ALO	52,372.17	89,347.06	64,734.54	7458.81	62,263.10
GWO	49,218.44	113,860.89	62,590.00	21,403.45	50,576.35
MFO	49,141.25	220,477.60	84,223.73	34,322.99	79,630.52
TLBO	49,504.24	80,344.96	56,061.12	5078.10	59,982.06

footing generally reduces the final cost. By increasing the depth of footing from 300 mm to 3000 mm, the cost of the foundation can be reduced by about 38%. Figure 5 shows mean values for all optimization methods as footing depth increases. BBO and WDE were successful in fesiable solution while other techniques did not converge in most of the cases. At depths greater than 1000 mm both the BBO and WDE showed monotonic variations in final designs; whereas, the other algorithms did not follow any pattern. The mean design generated by WDE is about 8.81% less than BBO.

Table 11 lists designs obtained from each optimization method as the compressive strength of the concrete varies from 20 to 55 MPa. As the compressive strength increase, the cost of the WDE and BBO designs decrease, with a maximum cost reduction of about 28%. Figure 6 shows the change in the cost of the foundation designs as concrete compressive strength decreases. BBO and WDE show consistent cost reductions as the concrete strength increase; whereas, the remaining algorithm do not demonstrate this effect or only sporadically.

Table 12 lists designs obtained by each method as the inclination angle changes from 0 to 40°. WDE results it can be observed that when the inclination angle is increased from 0° to 30° the final cost increase only slightly; however, after that the cost increases sharply with maximum cost increases 43.39% and 40.56% obtained by BBO and WDE, respectively. Figure 7 shows the mean results for all optimization methods as the inclination angle increases. The cost of BBO and WDE designs for inclination angles between 0° and 30° increase slightly; whereas; from 35° to 45° the cost increase about 40%.

Tables 13, 14, 15, and 16 demonstrate that design obtained by BBO and WDE were not very sensitivity to

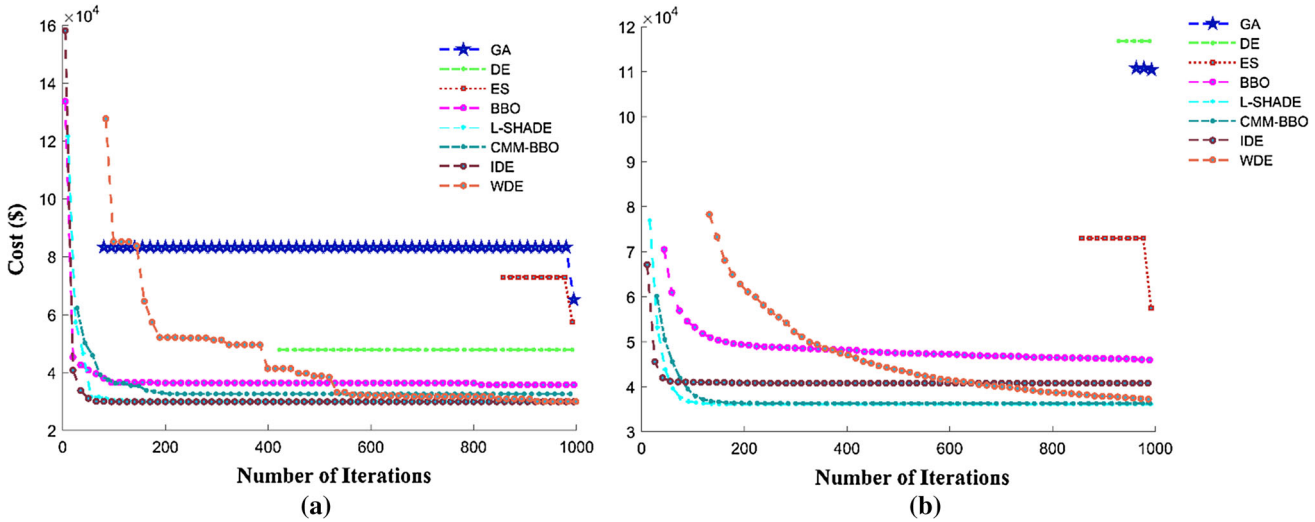

Fig. 4 Convergence history based on best-found solutions and mean results for Case I

various in the other input parameters (i.e., ϕ, γ, E_s, and υ). Comparison of the current results with the previous studies listed in Table 8 demonstrated that in terms of the best results WDE and BBO obtained lower cost designs than APSO, FA, WOA, and GWO. Based on the mean results BBO out performed PSO, APSO, FA, LKH, and WOA, while WDE was better than all the swarm algorithms expect of GWO and TLBO.

Figure 8 shows the convergence rate history for the best-found solutions and mean results and demonstrate that BBO and WDE significantly outperform IDE. A comparison of BBO and WDE shows that BBO found feasible solutions sooner than WDE and converged the its final design at the beginning of the search and varied slightly after that point. In contrary, WDE experienced many changes during the search process and converged to its final optimum solution after 600th iteration. Convergence history based on the mean results show WDE out performed BBO and that IDE did not work efficiently in this case. As discussed comprehensively and demonstrated in the results, by changing the loading conditions the objective function became more complex than Case I. Only three of the eight optimization algorithms, BBO, WDE, and IDE, were capable of solving this foundation problem. Furthermore. only WDE obtained feasible solution in 101 runs.

5.3 Case III: axial and flexural loading with dynamic location

In Case III, the location of the column is not fixed and can vary within the two-dimensional space at the top of the foundation. Therefore, two more design variables, the eccentricity of the column along with x and y directions, are added to foundation problem defined in Case II,. The most important effect of varying the location the column is moderating the pressure distribution under the footing and making it more uniform. which can prevent the foundation structure from having an unbalanced strength. The results listed in Tables 5 and 6 show that only BBO and WDE obtained feasible designs. BBO found the lowest cost design of $49,432.67 which is 8.92% less than WDE's. However, WDE recorded better overall results in terms of the worst, mean, SD, and median values. Furthermore, the results indicated the positive influence of including the

Table 9 Final level of construction operations and facilities for Case II

The resultant operations content	Unit	Value							
		GA	DE	ES	BBO	L-SHADE	CMM-BBO	IDE	WDE
Excavation	m^3	–	–	–	8.95	–	–	9.34	10.71
Concrete framework	m^2	–	–	–	6.87	–	–	5.68	6.87
Reinforcement	kg	–	–	–	3.77E+03	–	–	7.66E+03	3.77E+03
Concrete	m^3	–	–	–	4.39	–	–	2.81	4.39
Compacted backfill	m^3	–	–	–	1.77	–	–	2.26	2.12

Table 10 Cost ($) design variation under the varying depth of foundation for Case II

D_f (m)	GA	DE	ES	BBO	L-SHADE	CMM-BBO	IDE	WDE
300	N.G.	N.G.	N.G.	135,391.9	135,519.09	135,519.1	135,519.1	135,566.75
500	N.G.	N.G.	N.G.	114,385.1	115,076.56	115,076.6	115,076.6	115,111.74
700	119,154	N.G.	N.G.	97,367.43	99,249.10	99,249.1	99,249.1	99,265.26
800	N.G.	N.G.	106,361.2	91,182.49	89,523.20	89,523.2	89,523.2	89,602.53
1000	N.G.	108,867.6	130,212.5	82,581.76	N.G.	N.G.	N.G.	82,629.60
1200	208,411.2	131,832.2	142,731	82,642.55	N.G.	N.G.	169,788.1	83,129.53
1400	221,234.5	N.G.	N.G.	82,650.85	N.G.	N.G.	162,581.7	82,712.42
1600	N.G.	N.G.	94,106.75	82,707.39	N.G.	N.G.	168,097.4	82,698.75
1800	N.G.	211,061.2	109,024	82,756.66	N.G.	N.G.	N.G.	82,808.66
2000	115,739.3	192,416.6	117,986.2	82,785.29	N.G.	N.G.	168,162.7	82,802.18
2200	177,281	N.G.	116,324.1	82,850.05	N.G.	N.G.	168,452.7	82,861.07
2400	195,449.1	141,458	N.G.	82,874.55	N.G.	N.G.	163,771.4	82,962.48
2600	N.G.	109,287.1	N.G.	82,932.78	82,911.95	N.G.	N.G.	83,006.99
2800	N.G.	N.G.	183,062.1	82,994.54	N.G.	N.G.	N.G.	83,009.01
3000	207,476.4	N.G.	102,807.3	83,012.39	N.G.	N.G.	N.G.	83,197.67
Variation (%)	–	–	–	− 38.69	–	–	–	− 38.63

Table 11 Cost ($) design variation under varying compressive strength of concrete for Case II

f_c (MPa)	GA	DE	ES	BBO	L-SHADE	CMM-BBO	IDE	WDE
20	115,383.9	102,259.8	201,676.6	82,592.51	N.G.	N.G.	N.G.	83,392.64
25	N.G.	192,468	N.G.	76,023.51	77,293.38	N.G.	N.G.	75,986.84
30	118,075	103,926.3	85,542.49	72,407.65	72,221.42	N.G.	N.G.	72,244.33
35	113,412.9	113,663.9	90,179.59	68,394.72	68,301.68	N.G.	N.G.	68,341.25
40	123,813.3	N.G.	116,432	64,459.45	67,417.6	N.G.	N.G.	64,541.41
45	N.G.	N.G.	N.G.	62,298.45	N.G.	N.G.	N.G.	62,744.01
50	114,589.3	110,126.5	75,195.36	61,453.68	61,726.18	N.G.	N.G.	61,356.66
55	N.G.	N.G.	94,695.98	59,206.41	60,817.5	N.G.	N.G.	59,222.85
Variation (%)	–	–	− 53.05	− 28.32	–	–	–	− 28.98

location of the column as a design variable; reducing the cost of the foundation by nearly 40%.

Tables 6 and 17 list the values of the design variables and operational costs for best Case III foundation designs, respectively. BBO and WDE obtained feasible designs while GA, DE, ES, L-SHADE, CMM-BBO, and IDE were not successful. Comparison of the results with the previous study by Gandomi and Kashani (2018) demonstrated that LKH found the lowest best value while TLBO obtained the lowest of mean value.

Tables 18, 19, 20, 21, 22, 23, and 24 list the results of a sensitivity analysis of the effect of various soil parameters to the Case III final design based on the best and mean results of 101 runs. Figures 9, 10, and 11 shows a comparison of mean values for each optimization method for variations in the values of soil parameters.

The results in Table 18 show considerable change in the low-cost designs as Df varies from 300 mm to 3000 mm. Only BBO solved the problem efficiently, while the performance of other algorithms was varied sporadically. In general, the results demonstrated that increasing the depth of footing generally reduces the final cost. By increasing the depth of footing from 300 mm to 3000 mm, the cost of the foundation can be reduced by about 37%. Figure 9 shows mean values for all optimization methods as footing depth increases. Only BBO consistently obtained fesiable solutions while other techniques did not converge in most of the cases. At depths greater than 1600 mm, there was little effect on the final design due to depth.

Table 19 lists designs obtained from each optimization method as the compressive strength of the concrete varies

Table 12 Cost ($) design variation under varying effective force inclination with respect to the vertical direction for Case II

i (°)	GA	DE	ES	BBO	L-SHADE	CMM-BBO	IDE	WDE
0	91,299.71	145,499.5	106,163.7	82,662.71	85,776.54	N.G.	N.G.	82,953.95
5	123,446	N.G.	N.G.	82,647.22	N.G.	N.G.	N.G.	82,993.9
10	N.G.	188,159.7	N.G.	82,858.23	N.G.	N.G.	N.G.	82,704.1
15	N.G.	102,259.8	N.G.	82,739.62	N.G.	N.G.	N.G.	83,610.27
20	N.G.	N.G.	216,040.1	82,809.72	N.G.	N.G.	N.G.	83,349.46
25	N.G.	N.G.	N.G.	82,880.09	N.G.	N.G.	N.G.	83,726.1
30	N.G.	N.G.	N.G.	82,934.74	N.G.	N.G.	N.G.	83,730.37
35	N.G.	N.G.	N.G.	83,505.88	86,227.79	N.G.	N.G.	84,078.81
40	N.G.	N.G.	N.G.	98,917.09	90,292.52	N.G.	N.G.	92,756.58
45	N.G.	N.G.	N.G.	118,528.5	117,908.7	N.G.	N.G.	116,604.1
Variation (%)	–	–	–	43.39	–	–	–	40.56

Table 13 Cost ($) design variation under varying friction angle of base soil for Case II

φ (°)	GA	DE	ES	BBO	L-SHADE	CMM-BBO	IDE	WDE
28	N.G.	N.G.	N.G.	82,691.6	N.G.	N.G.	N.G.	82,786.74
30	N.G.	N.G.	109,633.9	82,600.74	N.G.	N.G.	N.G.	82,900.21
32	105,463.2	103,824.3	N.G.	82,524.3	N.G.	N.G.	N.G.	82,660.11
34	N.G.	194,759.1	99,036.07	82,475.24	N.G.	N.G.	N.G.	82,484.33
36	205,540.9	N.G.	105,803.9	82,399.66	N.G.	N.G.	N.G.	83,212.1
38	202,081.5	N.G.	N.G.	82,408.4	N.G.	N.G.	N.G.	82,538.07
Variation (%)	–	–	–	− 0.34	–	–	–	− 0.30

Table 14 Cost ($) design variation under varying soil density for Case II

γ (°)	GA	DE	ES	BBO	L-SHADE	CMM-BBO	IDE	WDE
11.5	105,480	135,606.5	N.G.	82,846.68	85,952.83	N.G.	N.G.	82,823.18
13.5	201,119.4	145,499.5	N.G.	82,701.82	N.G.	N.G.	N.G.	82,979.04
15.5	N.G.	213,012.5	112,991.4	82,694.44	N.G.	N.G.	N.G.	82,817.23
17.5	188,711.5	N.G.	N.G.	83,175.59	N.G.	N.G.	N.G.	83,509.75
19.5	N.G.	N.G.	N.G.	82,551.57	N.G.	N.G.	N.G.	82,597.49
21.5	202,081.5	121,366.8	183,820.3	82,619.57	N.G.	N.G.	N.G.	82,626.85
23.5	117,782.6	89,199.26	112,281.2	82,550.3	N.G.	N.G.	N.G.	82,847.11
Variation (%)	11.66	− 34.22	–	− 0.36	–	–	–	0.03

from 20 to 55 MPa. As the compressive strength increase, the cost of the BBO designs decrease, with a maximum cost reduction of about 69%. Figure 10 shows the change in the cost of the foundation designs as concrete compressive strength decreases. BBO show consistent cost reductions as the concrete strength increase; whereas, the remaining algorithm do not demonstrate this effect or only sporadically.

Table 20 lists designs obtained by each method as the inclination angle changes from 0 to 40°. That BBO, L-SHADE, and IDE results show that as the inclination angle is increased from 0° to 15° the final cost increase only slightly; however, after that the cost increases sharply with maximum cost increases 35.73%, 49.91%, and 47.81% obtained by BBO, L-SHADE, and IDE, respectively. Figure 11 shows the mean results for all optimization methods as the inclination angle increases. Th e cost of

Table 15 Cost ($) design variation under varying modulus of elasticity for Case II

E_s (kPa)	GA	DE	ES	BBO	L-SHADE	CMM-BBO	IDE	WDE
10,500	N.G.	N.G.	115,052.8	82,590.95	N.G.	N.G.	N.G.	82,644.07
20,500	215,781	N.G.	N.G.	82,593.03	N.G.	N.G.	N.G.	82,614.96
30,500	109,338	N.G.	191,171.5	82,573.05	N.G.	N.G.	N.G.	82,733.85
40,500	117,782.6	N.G.	N.G.	82,634.41	N.G.	N.G.	N.G.	82,640.13
50,500	201,119.4	N.G.	N.G.	82,557.94	N.G.	N.G.	N.G.	83,431.3
60,500	97,077.5	N.G.	99,036.07	82,576.97	N.G.	N.G.	N.G.	83,490.63
70,500	N.G.	N.G.	N.G.	82,653.84	N.G.	N.G.	N.G.	83,094.52
80,500	N.G.	217,417	108,009.9	82,570.73	N.G.	N.G.	N.G.	82,611.58
90,500	186,177.1	N.G.	97,177.59	82,616.26	83,335.72	N.G.	N.G.	82,697.69
Variation (%)	–	–	− 15.54	0.03	–	–	–	0.06

Table 16 Cost ($) design variation under varying Poisson's ratio for Case II

υ	GA	DE	ES	BBO	L-SHADE	CMM-BBO	IDE	WDE
0.1	N.G.	113,450.5	191,171.5	83,493.51	N.G.	N.G.	N.G.	82,635.82
0.2	92,686.72	N.G.	N.G.	82,765.3	N.G.	N.G.	N.G.	82,586.48
0.3	177,612.9	89,199.26	116,254.4	82,553.41	N.G.	N.G.	N.G.	82,696.31
0.4	177,487.3	111,385.9	N.G.	82,575.37	82,539.51	N.G.	N.G.	82,707.68
0.5	85,697.1	198,586.6	130,263.5	82,737.76	N.G.	N.G.	N.G.	82,739.22
0.6	85,697.1	185,961.7	N.G.	82,572.35	N.G.	N.G.	N.G.	83,361.62
0.7	N.G.	N.G.	N.G.	82,676.94	N.G.	N.G.	N.G.	82,762.3
0.8	N.G.	N.G.	116,254.4	82,661.18	N.G.	N.G.	N.G.	82,756.44
0.9	N.G.	N.G.	109,633.9	82,572.35	N.G.	N.G.	N.G.	82,652.39
1	177,487.3	192,531.8	N.G.	83,443.09	82,539.51	N.G.	N.G.	83,312.7
Variation (%)	–	69.71	− 0.01	− 0.06	–	N.G.	N.G.	0.82

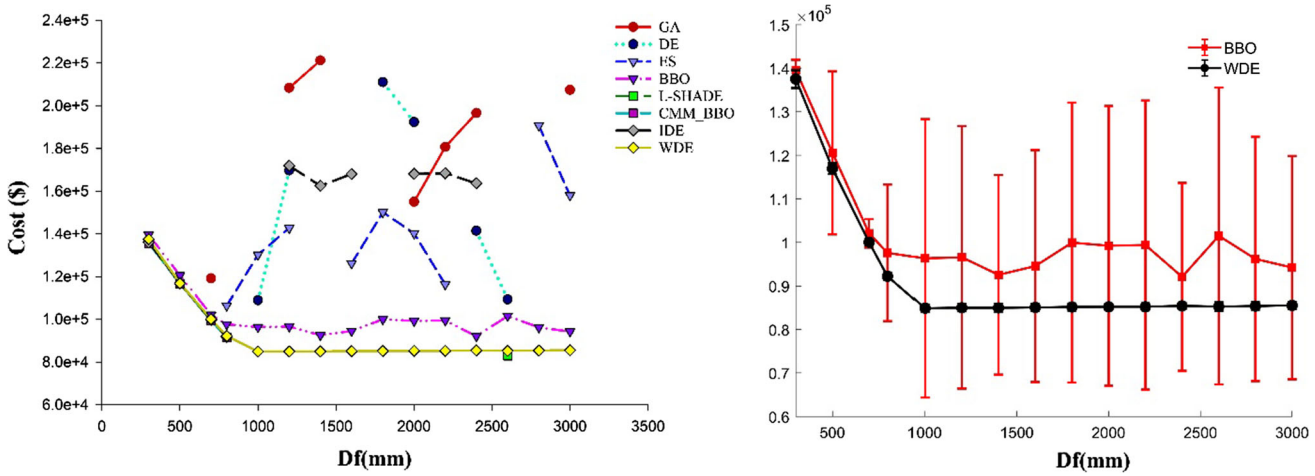

Fig. 5 Mean cost ($) design variation under the varying depth of foundation for Case II

L-SHADE designs for inclination angles between 0° and 35° increase slightly; whereas; from 35° to 45° the cost increase about 49%.

Table 20 lists designs obtained by each method as the inclination angle changes from 0 to 40°. that BBO, L-SHADE, and IDE results show that as the inclination angle is increased from 0° to 15° the final cost increase only slightly; however, after that the cost increases sharply with maximum cost increases 35.73%, 49.91%, and 47.81% obtained by BBO, L-SHADE, and IDE,

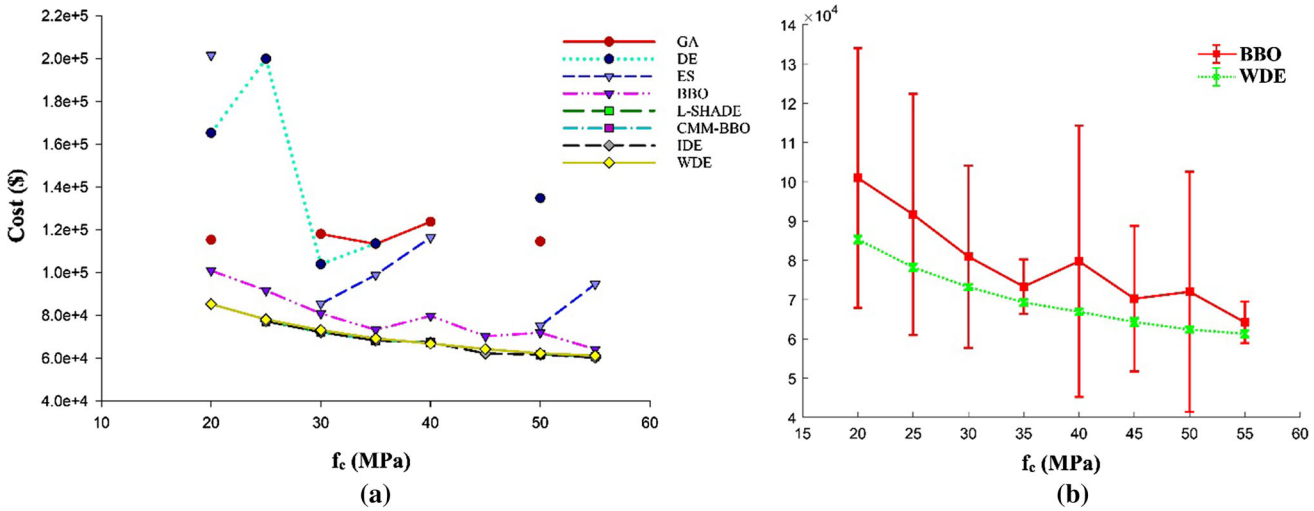

Fig. 6 Mean cost ($) design variation under varying compressive strength of concrete for Case II

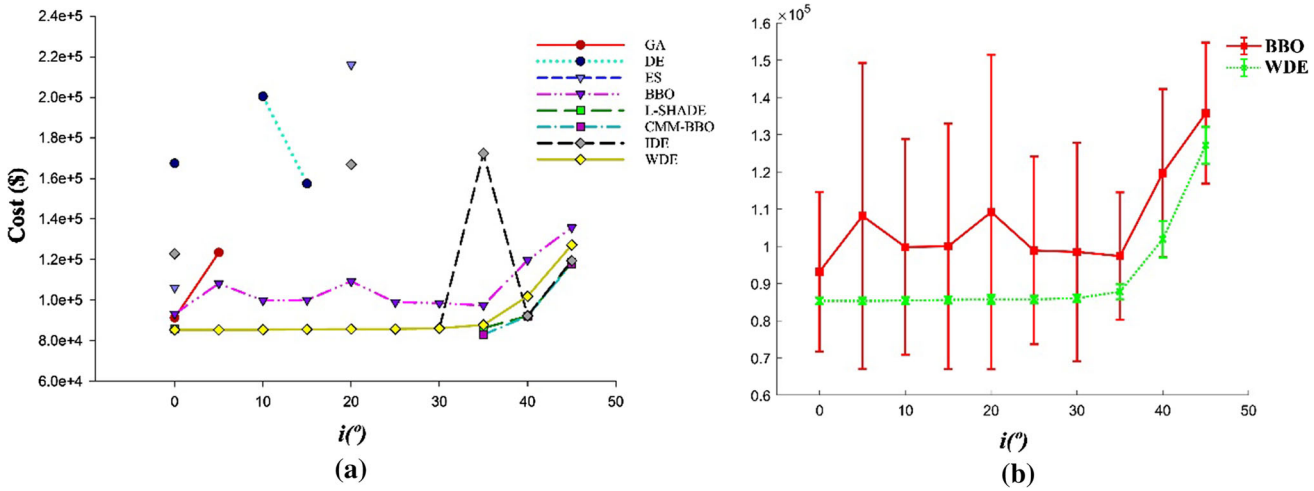

Fig. 7 Mean cost ($) design variation under varying effective force inclination with respect to the vertical direction for Case II

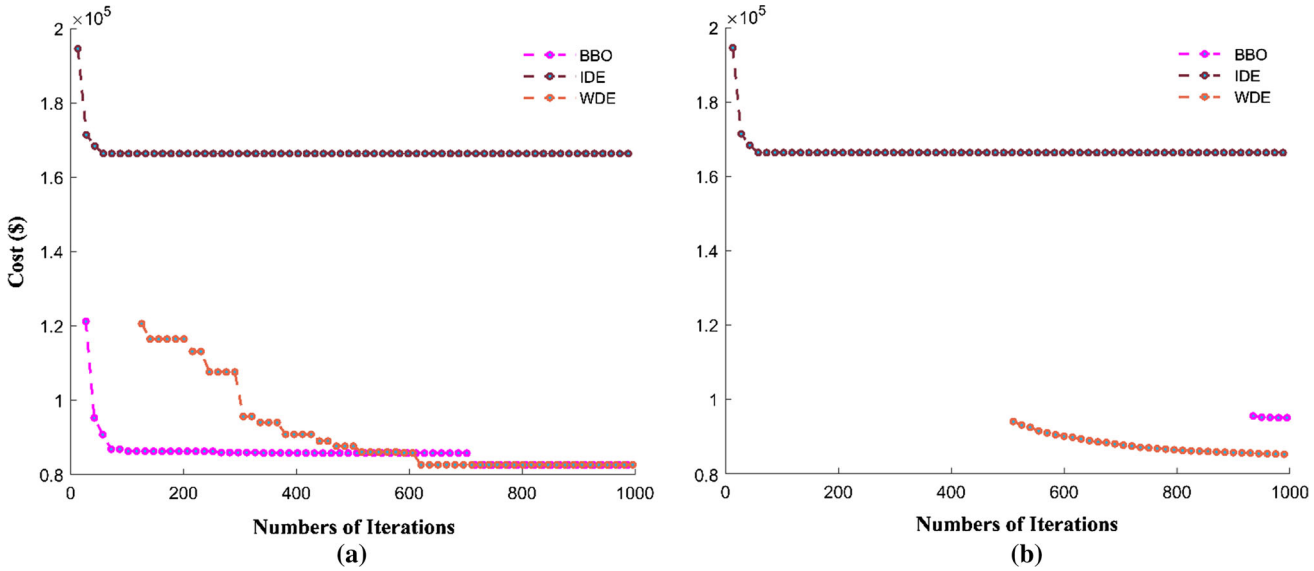

Fig. 8 Convergence history based on best-found solutions and mean results for Case II

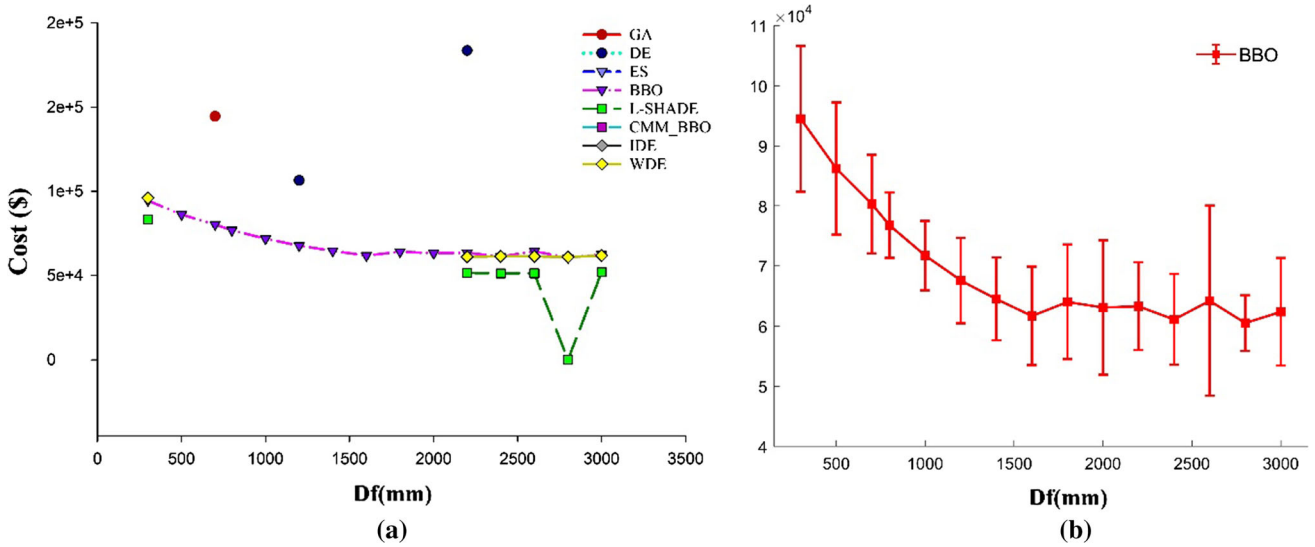

Fig. 9 Mean cost ($) design variation under the varying depth of foundation for Case III

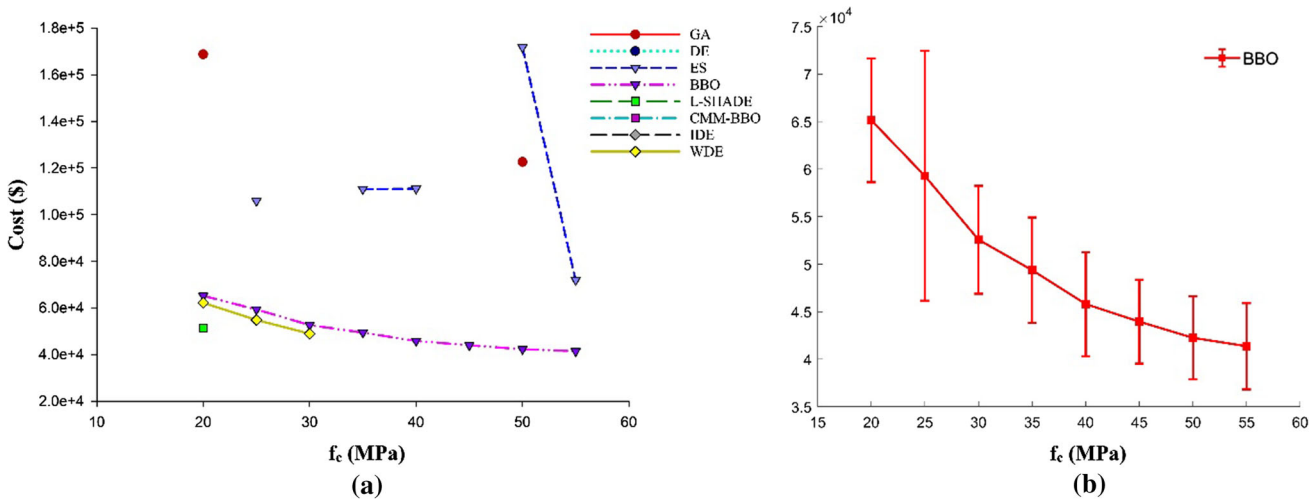

Fig. 10 Mean cost ($) design variation under varying compressive strength of concrete for Case III

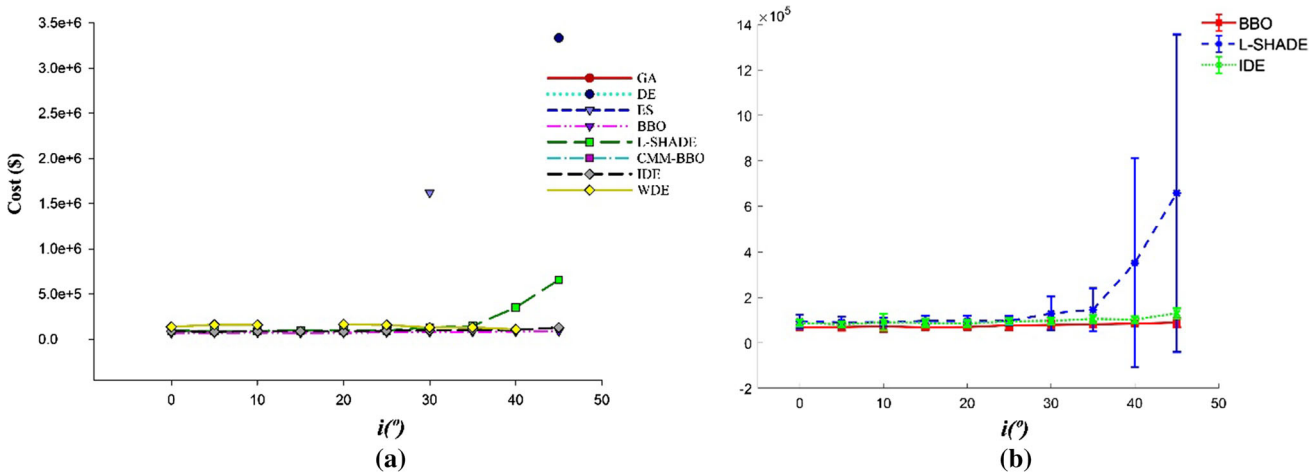

Fig. 11 Mean cost ($) design variation under varying effective force inclination with respect to the vertical direction for Case III

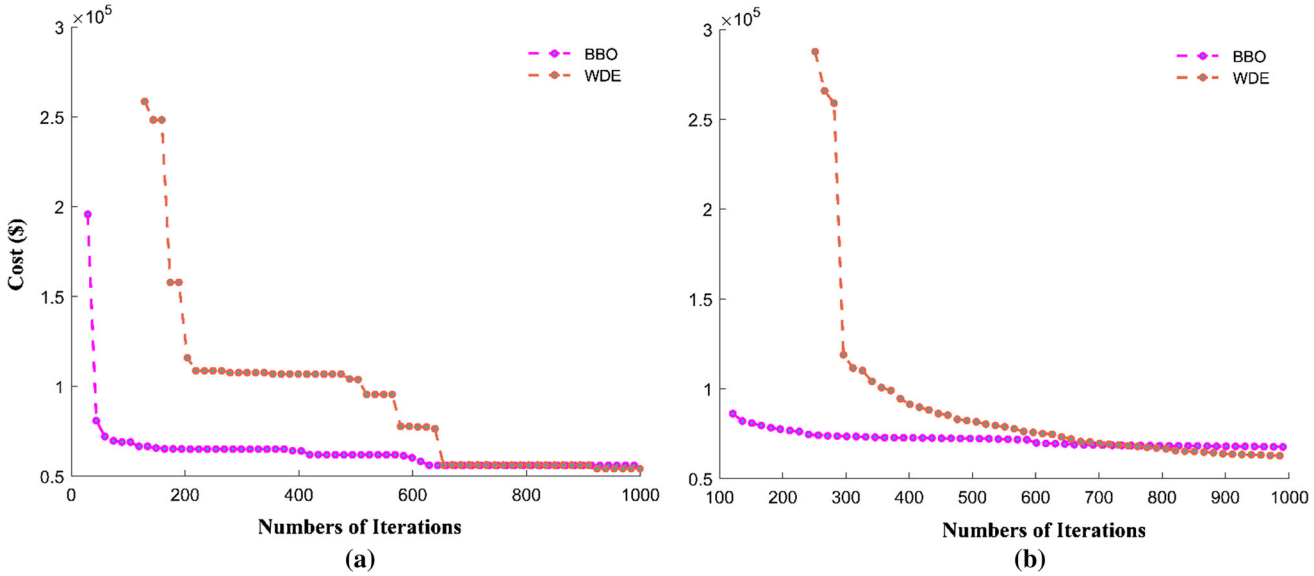

Fig. 12 Convergence history based on best-found solutions and mean results for Case III

respectively. Figure 11 shows the mean results for all optimization methods as the inclination angle increases. Th e cost of L-SHADE designs for inclination angles between 0° and 35° increase slightly; whereas; from 35° to 45° the cost increase about 49%.

Tables 21, 22, 23 and 24 demonstrate that obtained feasible designs were not very sensitivity to various in the other input parameters (i.e., ϕ, γ, E_s, and υ). Figure 12 shows the convergence rate history for the best-found solutions and mean results and demonstrate that BBO significantly outperform WDE. A comparison of BBO and WDE shows that BBO found feasible solutions sooner than WDE and converged the its final design at the initial steps (less than 200 iterations) and varied slightly after that point. In contrary, WDE experienced many changes during the search process and converged to its final optimum solution after 600th iteration. Convergence history based on the mean results again shows that BBO converged to feasible designs earlier than WDE. As demonstrated in the results, adding the location of the column as a design variable changes the objective function and becomes more complex than Case II. Only two of the eight optimization algorithms, BBO and WDE were capable of solving this foundation problem. Furthermore. only BBO obtained feasible solution in 101 runs.

6 Conclusions

The present study is devoted to examining the performance of three main evolutionary metaheuristic optimization algorithms (DE, ES, and BBO) and some of their successful variations (L-SHADE, CMM-BBO, IDE, and WDE) on cost optimization of a reinforced concrete shallow footing. In order to examine the performance of the mentioned algorithms, a MATLAB code is developed based on ACI 318-05 requirements. Low cost shallow foundation designs were generated for two loading cases: 1) a uniaxial force and 2) a combination of a uniaxial force and a flexural moment. In the third case, the location of the column along the top of the foundation is considered to a design variable. All the optimization algorithms are run 101 times, and the results reported in the form of best, worst, mean, SD, and median of successful runs. Results show that only BBO and WDE algorithms were able to deal successfully with all the cases. In fact, all the algorithms were successful in handling the first case; however, in the second case only7 BBO and WDE obtained feasible designs. Based on the best low cost designs, it was shown that that applying a flexural moment to the footing causes about a 176% increase in cost; whereas, allowing location of the column to vary on top of the footing reduces the cost about 40%. In summary, none of the presented optimization algorithms were successful for all cases. However, for Case I, L-SHADE obtained the lowest best and mean values. WDE and BBO provided the best design for Case II and Case III, respectively.

A sensitiveity analysis measured the cost of feasible foundation designs due changes in the following parameters: base soil friction angle from 28° to 38°, soil density from 11.5 to 23.5 kN/m^3, modulus of elasticity from 10,500 to 90,500 kPa, Poison's ratio from 0.1 to 1, concrete compressive strength from 20 to 55 MPa, effective force inclination respect to vertical axis from 0° to 45°, and depth of footing from 300 mm to 3000 mm. Variations of D_f, f_c,

Table 17 Final level of construction operations and facilities for Case III

The resultant operations content	Unit	Value							
		GA	DE	ES	BBO	L-SHADE	CMM-BBO	IDE	WDE
Excavation	m^3	–	–	–	10.95	–	–	–	11.54
Concrete framework	m^2	–	–	–	5.0095	–	–	–	5.44
Reinforcement	kg	–	–	–	2.23E+03	–	–	–	2.47 E+03
Concrete	m^3	–	–	–	2.60	–	–	–	2.86
Compacted backfill	m^3	–	–	–	2.58	–	–	–	2.70

Table 18 Cost ($) design variation under varying depth of foundation for Case III

D_f (m)	GA	DE	ES	BBO	L-SHADE	CMM-BBO	IDE	WDE
300	N.G.	N.G.	N.G.	82,092.04	N.G.	N.G.	N.G.	86,623.57
500	N.G.	N.G.	N.G.	71,436.18	N.G.	N.G.	N.G.	N.G.
700	144,547.4	N.G.	N.G.	66,709.61	N.G.	N.G.	N.G.	N.G.
800	N.G.	N.G.	N.G.	67,272.12	N.G.	N.G.	N.G.	N.G.
1000	N.G.	N.G.	N.G.	63,085.8	N.G.	N.G.	N.G.	N.G.
1200	N.G.	106,433.1	N.G.	58,458.99	N.G.	N.G.	N.G.	N.G.
1400	N.G.	N.G.	N.G.	55,841.72	N.G.	N.G.	N.G.	N.G.
1600	N.G.	N.G.	N.G.	51,560.36	N.G.	N.G.	N.G.	N.G.
1800	N.G.	N.G.	N.G.	51,045.92	N.G.	N.G.	N.G.	N.G.
2000	N.G.	N.G.	N.G.	51,681.57	N.G.	N.G.	N.G.	N.G.
2200	N.G.	133,501.4	N.G.	50,936.83	N.G.	N.G.	N.G.	53,710.9
2400	N.G.	N.G.	N.G.	50,944.72	N.G.	N.G.	N.G.	55,637.56
2600	N.G.	N.G.	N.G.	52,760.58	N.G.	N.G.	N.G.	55,131.87
2800	N.G.	N.G.	N.G.	50,911.85	N.G.	N.G.	N.G.	55,076.39
3000	N.G.	N.G.	N.G.	51,192.12	N.G.	N.G.	N.G.	51,629.04
Variation (%)	–	–	–	− 37.64	–	–	–	–

Table 19 Cost ($) design variation under varying compressive strength of concrete for Case III

f_c (MPa)	GA	DE	ES	BBO	L-SHADE	CMM-BBO	IDE	WDE
20	168,784.5	N.G.	N.G.	51,991.54	N.G.	N.G.	N.G.	53,925.02
25	N.G.	N.G.	105,855.2	46,068.64	N.G.	N.G.	N.G.	48,602.77
30	N.G.	N.G.	N.G.	44,060.38	N.G.	N.G.	N.G.	46,724.59
35	N.G.	N.G.	110,931.9	39,801.31	N.G.	N.G.	N.G.	N.G.
40	N.G.	N.G.	111,189.6	36,386.25	N.G.	N.G.	N.G.	N.G.
45	N.G.	N.G.	N.G.	35,763.86	N.G.	N.G.	N.G.	N.G.
50	122,588.4	N.G.	171,781.1	35,687.58	N.G.	N.G.	N.G.	N.G.
55	N.G.	N.G.	71,929.68	34,305.3	N.G.	N.G.	N.G.	N.G.
Variation (%)	–	–	–	− 69.15	–	–	–	–

and i had considerable impact on the final design cost. Based on these results the cost of a foundation was reduced by increasing the depth of footing from 300 mm to 1200 mm for Case II and by increasing the depth from 300 mm to 1800 mm for Case III. Using stronger concrete also resulted in a low cost designs. However, changing the effective force inclination angle with respect to the vertical direction from 15° to 45° increased the cost for both Cases II and III. Other mentioned input parameters had insignificant effects on the final designs.

Table 20 Cost ($) design variation under varying effective force inclination with respect to the vertical direction for Case III

i (°)	GA	DE	ES	BBO	L-SHADE	CMM-BBO	IDE	WDE
0	N.G.	N.G.	N.G.	56,442.04	59,928.89	N.G.	64,612.95	N.G.
5	N.G.	N.G.	N.G.	54,588.8	61,298.61	N.G.	60,157.71	N.G.
10	N.G.	N.G.	N.G.	54,187.8	62,915.01	N.G.	68,546.14	N.G.
15	N.G.	N.G.	N.G.	51,928.71	64,035.97	N.G.	66,405.02	N.G.
20	N.G.	N.G.	N.G.	57,339.86	70,318.04	N.G.	62,487.87	N.G.
25	N.G.	126,536.2	N.G.	61,231.49	66,151.91	N.G.	77,032.93	N.G.
30	N.G.	N.G.	N.G.	64,729.46	71,599.61	N.G.	75,984.31	N.G.
35	N.G.	N.G.	N.G.	68,699.79	83,805.42	N.G.	77,904.68	N.G.
40	N.G.	N.G.	N.G.	71,510.76	79,746.21	N.G.	84,467.11	N.G.
45	N.G.	N.G.	N.G.	76,610.07	89,840.11	N.G.	95,555.55	N.G.
Variation (%)	–	–	–	35.73	49.91	–	47.89	–

Table 21 Cost ($) design variation under varying friction angle of base soil for Case III

φ (°)	GA	DE	ES	BBO	L-SHADE	CMM-BBO	IDE	WDE
28	N.G.	N.G.	N.G.	52,695.49	64,678.39	N.G.	63,259.73	N.G.
30	N.G.	N.G.	N.G.	55,047.71	58,104.73	N.G.	63,311.59	130,197.3
32	N.G.	231,718	N.G.	54,350.52	85,064.69	N.G.	67,519.83	118,025.5
34	N.G.	N.G.	N.G.	52,792.72	N.G.	N.G.	62,109.73	115,106.5
36	N.G.	N.G.	N.G.	55,159.68	N.G.	N.G.	61,021.06	128,731.7
38	185,589.2	N.G.	N.G.	51,143.69	N.G.	N.G.	69,164.85	120,612.8
Variation (%)	–	–	–	− 2.94	–	–	9.33	–

Table 22 Cost ($) design variation under varying soil density for Case III

γ (°)	GA	DE	ES	BBO	L-SHADE	CMM-BBO	IDE	WDE
11.5	N.G.	N.G.	N.G.	56,505.33	69,159.45	N.G.	61,156.05	N.G.
13.5	N.G.	231,718	N.G.	55,043.18	57,354.19	N.G.	64,498.02	N.G.
15.5	N.G.	115,166.4	163,118.2	56,036.58	67,782.45	N.G.	62,578.5	N.G.
17.5	N.G.	N.G.	N.G.	50,249.32	55,311.28	N.G.	62,327.23	N.G.
19.5	N.G.	N.G.	N.G.	55,190.71	66,264.3	N.G.	68,251.97	N.G.
21.5	N.G.	N.G.	N.G.	50,410.93	82,232.17	N.G.	66,774.31	N.G.
23.5	N.G.	N.G.	161,874.6	52,764.79	75,812.09	N.G.	62,055.69	N.G.
Variation (%)	–	–	–	− 6.62	9.62	–	1.47	–

Table 23 Cost ($) design variation under varying modulus of elasticity for Case III

E_s (kPa)	GA	DE	ES	BBO	L-SHADE	CMM-BBO	IDE	WDE
10,500	N.G.	N.G.	N.G.	N.G.	68,976.09	N.G.	69,248.58	N.G.
20,500	N.G.	112,810.2	132,913.8	N.G.	61,052.41	N.G.	70,868.36	N.G.
30,500	N.G.	140,066.4	154,343.7	N.G.	61,376.15	N.G.	63,501.42	N.G.
40,500	N.G.	N.G.	N.G.	N.G.	59,424.4	N.G.	63,478.81	N.G.
50,500	N.G.	N.G.	N.G.	N.G.	61,560.54	N.G.	60,865.56	N.G.
60,500	191,740.5	151,938.4	176,960.5	N.G.	65,669.32	N.G.	71,845.7	N.G.
70,500	N.G.	N.G.	N.G.	N.G.	61,997.06	N.G.	76,172.53	N.G.
80,500	164,477.5	117,382.1	N.G.	N.G.	62,491.87	N.G.	62,253.54	N.G.
90,500	69,706.2	N.G.	117,875.2	N.G.	67,142.64	N.G.	68,955.79	N.G.
Variation (%)	–	–	–	–	− 2.66	–	− 0.42	–

Table 24 Cost ($) design variation under varying Poisson's ratio for Case III

υ	GA	DE	ES	BBO	L-SHADE	CMM-BBO	IDE	WDE
0.1	N.G.	N.G.	N.G.	55,526.56	61,626.69	N.G.	67,176.87	N.G.
0.2	N.G.	N.G.	N.G.	55,090.37	68,549.29	N.G.	62,777.75	N.G.
0.3	N.G.	N.G.	230,295.8	53,417.51	69,490.95	N.G.	63,407.87	N.G.
0.4	N.G.	138,621.5	126,826.5	51,556.77	64,930.66	N.G.	67,283.73	N.G.
0.5	N.G.	N.G.	139,430.8	56,064.53	65,281.11	N.G.	64,052.58	N.G.
0.6	N.G.	N.G.	N.G.	52,355.02	64,217.18	N.G.	67,016.08	N.G.
0.7	N.G.	N.G.	N.G.	52,510.76	60,553.25	N.G.	66,744.65	N.G.
0.8	157,226.2	157,014.2	N.G.	55,385.74	59,346.11	N.G.	63,311.59	N.G.
0.9	N.G.	N.G.	N.G.	54,891.05	63,240.32	N.G.	64,070.91	N.G.
1	241,104.4	131,863.9	N.G.	54,891.05	67,686.63	N.G.	67,116.53	N.G.
Variation (%)	–	–	–	− 1.14	9.83	–	− 0.09	–

Funding Authors confirm that there is no funding support for this study.

Compliance with ethical standards

Conflict of interest Authors declare that they have no conflict of interest.

Human and animal rights This article does not contain any studies with human participants or animals performed by any of the authors.

References

Abbasnia R, Hosseinpour F, Rostamian M, Ziaadiny H (2012) Effect of corner radius on stress–strain behavior of FRP confined prisms under axial cyclic compression. Eng Struct 40:529–535

Abbasnia R, Hosseinpour F, Rostamian M, Ziaadiny H (2013) Cyclic and monotonic behavior of FRP confined concrete rectangular prisms with different aspect ratios. Constr Build Mater 40:118–125

Akhani M, Kashani AR, Mousavi M, Gandomi AH (2019) A hybrid computational intelligence approach to predict spectral acceleration. Measurement 138:578–589

Algin HM (2009) Elastic settlement under eccentrically loaded rectangular surface footings on sand deposits. J Geotech Geoenviron Eng 135(10):1499–1508

American Concrete Institute (2005) Building code requirements for structural concrete and commentary (ACI 318-05), Detroit

Arab HG, Rashki M, Rostamian M, Ghavidel A, Shahraki H, Keshtegar B (2018) Refined first-order reliability method using cross-entropy optimization method. Eng Comput 1–13

Aydogdu I (2017) Cost optimization of reinforced concrete cantilever retaining walls under seismic loading using a biogeography-based optimization algorithm with Levy flights. Eng Optim 49(3):381–400

Aydoğdu İ, Akın A, Saka MP (2016) Design optimization of real world steel space frames using artificial bee colony algorithm with Levy flight distribution. Adv Eng Softw 92:1–14

Azizi K, Attari J, Moridi A (2017) Estimation of discharge coefficient and optimization of Piano Key Weirs. In: Labyrinth and Piano Key Weirs III: proceedings of the 3rd international workshop on Labyrinth and Piano Key Weirs (PKW 2017), February 22–24, 2017, Qui Nhon, Vietnam. CRC Press, p 213

Brownlee J (2011) Clever algorithms: nature-inspired programming recipes

Camp CV, Akin A (2011) Design of retaining walls using big bang–big crunch optimization. J Struct Eng 138(3):438–448

Camp CV, Assadollahi A (2013) CO_2 and cost optimization of reinforced concrete footings using a hybrid big bang-big crunch algorithm. Struct Multidiscip Optim 48(2):411–426

Camp CV, Assadollahi A (2015) CO_2 and cost optimization of reinforced concrete footings subjected to uniaxial uplift. J Build Eng 3:171–183

Çarbaş S (2017) Optimum structural design of spatial steel frames via biogeography-based optimization. Neural Comput Appl 28(6):1525–1539

Celikoglu HB (2013) An approach to dynamic classification of traffic flow patterns. Comput Aided Civ Infrastruct Eng 28(4):273–288

Chen X, Tianfield H, Du W, Liu G (2016) Biogeography-based optimization with covariance matrix based migration. Appl Soft Comput 45:71–85

Cheng MY, Tran DH, Hoang ND (2017) Fuzzy clustering chaotic-based differential evolution for resource leveling in construction projects. J Civ Eng Manag 23(1):113–124

Civicioglu P, Besdok E, Gunen MA, Atasever UH (2018) Weighted differential evolution algorithm for numerical function optimization: a comparative study with cuckoo search, artificial bee colony, adaptive differential evolution, and backtracking search optimization algorithms. Neural Comput Appl 1–15

Darwin C (1859) The origin of species. Reprint. Modern Library, New York

Derakhshan S, Bashiri M (2018) Investigation of an efficient shape optimization procedure for centrifugal pump impeller using eagle strategy algorithm and ANN (case study: slurry flow). Struct Multidiscipl Optim 58(2):459–473

Elyasigomari V, Lee DA, Screen HRC, Shaheed MH (2017) Development of a two-stage gene selection method that incorporates a novel hybrid approach using the cuckoo optimization algorithm and harmony search for cancer classification. J Biomed Inform 67:11–20

Fister I, Gandomi AH, Fister IJ, Mousavi M, Farhadi A (2014) Soft computing in earthquake engineering: a short overview. Int J Earthq Eng Hazard Mitig 2(2):42–48

Franco G, Betti R, Luş H (2004) Identification of structural systems using an evolutionary strategy. J Eng Mech 130(10):1125–1139

Gandomi AH, Kashani AR (2016) Evolutionary bound constraint handling for particle swarm optimization. In: 2016 4th International symposium on computational and business intelligence (ISCBI). IEEE, pp 148–152
Gandomi AH, Kashani AR (2018) Construction cost minimization of shallow foundation using recent swarm intelligence techniques. IEEE Trans Ind Inform 14(3):1099–1106
Gandomi AH, Yang XS, Talatahari S, Alavi AH (eds) (2013) Metaheuristic applications in structures and infrastructures. Newnes, Oxford
Gandomi AH, Kashani AR, Mousavi M (2015) Boundary constraint handling affection on slope stability analysis. In: Lagaros ND, Papadrakakis M (eds) Engineering and applied sciences optimization. Springer, Basel, pp 341–358
Gandomi AH, Kashani AR, Roke DA, Mousavi M (2017a) Optimization of retaining wall design using evolutionary algorithms. Struct Multidiscipl Optim 55(3):809–825
Gandomi AH, Kashani AR, Mousavi M, Jalalvandi M (2017b) Slope stability analysis using evolutionary optimization techniques. Int J Numer Anal Meth Geomech 41(2):251–264
Gandomi AH, Kashani AR, Zeighami F (2017c) Retaining wall optimization using interior search algorithm with different bound constraint handling. Int J Numer Anal Methods Geomech. https://doi.org/10.1002/nag.2678
García-Segura T, Yepes V, Alcalá J (2017) Computer-support tool to optimize bridges automatically. Int J Comput Methods Exp Meas 5(2):171–178
Ghoddousi P, Javid AAS, Sobhani J (2015) A fuzzy system methodology for concrete mixture design considering maximum packing density and minimum cement content. Arab J Sci Eng 40(8):2239–2249
Ghoddousi P, Javid AAS, Sobhani J, Alamdari AZ (2016) A new method to determine initial setting time of cement and concrete using plate test. Mater Struct 49(8):3135–3142
Gholizadeh S, Poorhoseini H (2016) Seismic layout optimization of steel braced frames by an improved dolphin echolocation algorithm. Struct Multidiscip Optim 54(4):1011–1029
Hancer E, Karaboga D (2017) A comprehensive survey of traditional, merge-split and evolutionary approaches proposed for determination of cluster number. Swarm Evolut Comput 32:49–67
Holland JH (1975) Adaptation in natural and artificial systems. The University of Michigan Press, Ann Arbor
Ho-Huu V, Vo-Duy T, Luu-Van T, Le-Anh L, Nguyen-Thoi T (2016) Optimal design of truss structures with frequency constraints using improved differential evolution algorithm based on an adaptive mutation scheme. Autom Constr 68:81–94
Homaifar A, Lai SHY, Qi X (1994) Constrained optimization via genetic algorithms. Simulation 62(4):242–254
Ide T, Kitajima H, Otomori M, Leiva JP, Watson BC (2016) Structural optimization methods of nonlinear static analysis with contact and its application to design lightweight gear box of automatic transmission of vehicles. Struct Multidiscip Optim 53(6):1383–1394
Jalili S, Hosseinzadeh Y, Taghizadieh N (2016) A biogeography-based optimization for optimum discrete design of skeletal structures. Eng Optim 48(9):1491–1514
Kashani AR, Gandomi AH, Mousavi M (2016) Imperialistic competitive algorithm: a metaheuristic algorithm for locating the critical slip surface in 2-dimensional soil slopes. Geosci Front 7(1):83–89
Kashani AR, Saneirad A, Gandomi AH (2019) Optimum design of reinforced earth walls using evolutionary optimization algorithms. Neural Comput Appl 1–24
Kaveh A (2017) Damage detection in skeletal structures based on CSS optimization using incomplete modal data. In: Kaveh A (ed) Applications of metaheuristic optimization algorithms in civil engineering. Springer, Berlin, pp 201–211
Khajehzadeh M, Taha MR, El-Shafie A, Eslami M (2011) Modified particle swarm optimization for optimum design of spread footing and retaining wall. J Zhejiang Univ Sci A 12(6):415–427
Khajehzadeh M, Taha MR, El-Shafie A, Eslami M (2012) Optimization of shallow foundation using gravitational search algorithm. Res J Appl Sci Eng Technol 4:1124–1130
Khajehzadeh M, Taha MR, Eslami M (2013) A new hybrid firefly algorithm for foundation optimization. Natl Acad Sci Lett 36(3):279–288
Khoshroo M, Javid AAS, Katebi A (2018) Effects of micro-nano bubble water and binary mineral admixtures on the mechanical and durability properties of concrete. Constr Build Mater 164:371–385
Kumar S, Tejani GG, Mirjalili S (2018) Modified symbiotic organisms search for structural optimization. Eng Comput 1–28
Lee HG, Yi CY, Lee DE, Arditi D (2015) An advanced stochastic time-cost tradeoff analysis based on a CPM-guided genetic algorithm. Comput Aided Civ Infrastruct Eng 30:824–842
Mavrovouniotis M, Li C, Yang S (2017) A survey of swarm intelligence for dynamic optimization: Algorithms and applications. Swarm Evol Comput 33:1–17
Marinakis Y, Migdalas A, Sifaleras A (2017) A hybrid particle swarm optimization-variable neighborhood search algorithm for constrained shortest path problems. Eur J Oper Res 261(3):819–834
McCall AJ, Balling RJ (2017) Structural analysis and optimization of tall buildings connected with skybridges and atria. Struct Multidiscip Optim 55(2):583–600
Meng T, Pan QK (2017) An improved fruit fly optimization algorithm for solving the multidimensional knapsack problem. Appl Soft Comput 50:79–93
Meyerhof GG (1963) Some recent research on the bearing capacity of foundations. Can Geotech J 1(1):16–26
Molina-Moreno F, García-Segura T, Martí JV, Yepes V (2017) Optimization of buttressed earth-retaining walls using hybrid harmony search algorithms. Eng Struct 134:205–216
Mousavi M, Azarbakht A, Rahpeyma S, Farhadi A (2015) On the application of genetic programming for new generation of ground motion prediction equations. In: Gandomi AH, Alavi AH, Ryan C (eds) Handbook of genetic programming applications. Springer, Cham, pp 289–307
Nikbakht H, Papakonstantinou KG (2019) A direct Hamiltonian MCMC approach for reliability estimation. In: UNCECOMP 2019 - The 3rd international conference on uncertainty quantification in computational sciences and engineering, Crete, Greece, 24–26 June 2019
Omrani R, Kattan L (2013) Simultaneous calibration of microscopic traffic simulation model and estimation of origin/destination (OD) flows based on genetic algorithms in a high-performance computer. In: 2013 16th International IEEE conference on intelligent transportation systems-(ITSC). IEEE, pp 2316–2321
Omranian E, Abdelnaby A, Abdollahzadeh G, Rostamian M, Hosseinpour F (2018) Fragility curve development for the seismic vulnerability assessment of retrofitted RC bridges under mainshock-aftershock seismic sequences. In: Proceedings of the structures congress
Padhye N, Bhardawaj P, Deb K (2013) Improving differential evolution through a unifiedapproach. J Glob Optim 55:771–799. https://doi.org/10.1007/s10898-012-9897-0
Rashki M, Azarkish H, Rostamian M, Bahrpeyma A (2019) Classification correction of polynomial response surface methods for accurate reliability estimation. Struct Saf 81:101869
Pant M, Thangaraj R, Grosan C, Abraham A (2008) Hybrid differential evolution-particle swarm optimization algorithm for solving global optimization problems. In Third international

conference on digital information management, ICDIM 2008. IEEE, pp 18–24
Rechenberg I (1965) Cybernetic solution path of an experimental problem. Royal Aircraft Establishment, Farnborough, Library Translation, p 1122
Rostamian M, Abbasnia R, Zakeri JA, Amiri GG (2011) Investigation of stress–strain behavior of FRP confined concrete columns under compressive loading. Iran University of Science and Technology
Schwefel H-P (1977) Numeriche Optimierung von Computer-Modelen constructing genetic linkage maps of experimental and natural Mittels der Evolutions-Strategie. Birkauser, Basel
Seyedpoor SM, Shahbandeh S, Yazdanpanah O (2015) An efficient method for structural damage detection using a differential evolution algorithm-based optimisation approach. Civ Eng Environ Syst 32(3):230–250
Shayanfar M, Rostamian M, Ghanooni-Bagha M, Tajban A, Nemati S (2018) Evaluating the plasticity of concrete beam-column connections reinforced with FRP composite rebars. Eng Solid Mech 6(4):331–340
Simon D (2008) Biogeography-based optimization. IEEE Trans Evol Comput 12:702–713
Storn R, Price K (1997) Differential evolution: a simple and efficient heuristic for global optimization over continuous spaces. J Glob Optim 11(4):341–359
Tanabe R, Fukunaga A (2014) Improving the search performance of SHADE using linear population size reduction. In: Proc. IEEE congress on evolutionary computation. Bejing, pp 1658–1665
Tejani GG, Pholdee N, Bureerat S, Prayogo D (2018a) Multiobjective adaptive symbiotic organisms search for truss optimization problems. Knowl Based Syst 161:398–414
Tejani GG, Savsani VJ, Patel VK, Mirjalili S (2018b) Truss optimization with natural frequency bounds using improved symbiotic organisms search. Knowl Based Syst 143:162–178
Tejani GG, Savsani VJ, Patel VK, Savsani PV (2018c) Size, shape, and topology optimization of planar and space trusses using mutation-based improved metaheuristics. J Comput Des Eng 5(2):198–214
Tejani GG, Pholdee N, Bureerat S, Prayogo D, Gandomi AH (2019) Structural optimization using multi-objective modified adaptive symbiotic organisms search. Expert Syst Appl 125:425–441
Wallace AR (1876) The geographical distribution of animals: with a study of the relations of living and extinct faunas as elucidating the past changes of the earth's surface—in two volumes. Macmillan & Co, London
Wang Y (2009) Reliability-based economic design optimization of spread foundations. J Geotech Geoenviron Eng 135(7):954–959
Wang Y, Kulhawy FH (2008) Economic design optimization of foundations. J Geotech Geoenviron Eng 134(8):1097–1105
Yang XS, Gandomi AH, Talatahari S, Alavi AH (eds) (2012) Metaheuristics in water, geotechnical and transport engineering. Newnes, Oxford
Yang XS, Bekdaş G, Nigdeli SM (2016) Metaheuristics and optimization in civil engineering. In: Kuznetsov YA, Pironneau O, Neittaanmäki P (eds) Modeling and optimization in science and technologies, vol 7. Springer, Basel
Zeng F, Xie H, Liu Q, Li F, Tan W (2016) Design and optimization of a new composite bumper beam in high-speed frontal crashes. Struct Multidiscip Optim 53(1):115–122
Zhang J, Sanderson AC (2009) JADE: Adaptive Differential Evolution with optional external archive. IEEE Trans Evol Comput 13(5):945–958
Zhao BD, Zhang LL, Jeng DS, Wang JH, Chen JJ (2015) Inverse analysis of deep excavation using differential evolution algorithm. Int J Numer Anal Methods Geomech 39(2):115–134
Zhou G, Ma ZD, Gu J, Li G, Cheng A, Zhang W (2016) Design optimization of a NPR structure based on HAM optimization method. Struct Multidiscip Optim 53(3):635–643